AD_____

Award Number: W81XWH-10-1-0176

TITLE: Suppression of BRCA2 by Mutant Mitochondrial DNA in Prostate Cancer

PRINCIPAL INVESTIGATOR: Jer-Tsong Hsieh

CONTRACTING ORGANIZATION: University of Texas Southwestern Medical Center
Dallas, TX 75390

REPORT DATE: July 2014

TYPE OF REPORT: final

PREPARED FOR: U.S. Army Medical Research and Materiel Command
Fort Detrick, Maryland 21702-5012

REPORT DOCUMENTATION PAGE

Form Approved
OMB No. 0704-0188

1. REPORT DATE	2. REPORT TYPE	3. DATES COVERED
July 2014	Final	1 MAY 2010 - 30 APR 2014

4. TITLE AND SUBTITLE
Suppression of BRCA2 by Mutant Mitochondrial DNA in Prostate Cancer

5a. CONTRACT NUMBER

5b. GRANT NUMBER
W81XWH-10-1-0176

5c. PROGRAM ELEMENT NUMBER

6. AUTHOR(S)
Jer-Tsong Hsieh

E-Mail: jt.hsieh@utsouthwestern.edu

5d. PROJECT NUMBER

5e. TASK NUMBER

5f. WORK UNIT NUMBER

7. PERFORMING ORGANIZATION NAME(S) AND ADDRESS(ES)

University of Texas Southwestern Medical Center
Dallas, TX 75390

8. PERFORMING ORGANIZATION REPORT NUMBER

9. SPONSORING / MONITORING AGENCY NAME(S) AND ADDRESS(ES)
U.S. Army Medical Research and Materiel Command
Fort Detrick, Maryland 21702-5012

10. SPONSOR/MONITOR'S ACRONYM(S)

11. SPONSOR/MONITOR'S REPORT NUMBER(S)

12. DISTRIBUTION / AVAILABILITY STATEMENT
Approved for Public Release; Distribution Unlimited

13. SUPPLEMENTARY NOTES

14. ABSTRACT
Mutations in mitochondrial DNA (mtDNA) are frequent in prostate cancer and they seem to occur early during prostate malignant transformation. Depletion of mtDNA in prostate cancer cells has been linked to acquisition of androgen-independence, progression to an invasive phenotype that is resistant to conventional chemotherapies, as well as induction of epithelial-mesenchymal transition leading to cancer metastasis. Using long-range genomic polymerase chain reaction, large deletion of mtDNA can be detected in prostate cancer tissues but not benign or normal prostate tissues. Noticeably, our study excludes the germ-line origin of the mutant mtDNA pattern in prostate cancer patient through analysis of the blood of the corresponding patient. Our data conclude that mtDNA deletion is due to carcinogenesis process in somatic prostate cells.
In addition, our data have unveiled the molecular alteration in prostate cancer cells resulted from mtDNA deletion. For example, Skp2 protein elevation is often associated in prostate cells with loss of mtDNA. Also, the presence of Skp2 expression can decrease the expression of BRCA2 protein as an early biomarker of prostate neoplastic transformation, which is due to BRCA2 proteolysis.

15. SUBJECT TERMS

16. SECURITY CLASSIFICATION OF:			17. LIMITATION OF ABSTRACT	18. NUMBER OF PAGES	19a. NAME OF RESPONSIBLE PERSON
a. REPORT	b. ABSTRACT	c. THIS PAGE			19b. TELEPHONE NUMBER *(include area code)*
U	U	U	UU	40	USAMRMC

Table of Contents

INTRODUCTION

The development of newly effective strategies in the prevention and therapy of prostate carcinoma relies heavily upon increasing our knowledge of the interplay among various molecular alterations that lead to onset and progression of prostate cancer. At present, most of our knowledge pertains to defects resulting from genetic abnormalities in nuclear DNA-encoded genes, but it has also been recognized that cancer cells may harbor somatic or germline mutations affecting mitochondrial DNA (mtDNA) as well as depletion of the mtDNA content [1-3].

Mitochondrial DNA depletion has been shown to promote malignant progression of prostate cancer cells [4-6]. However, the molecular mechanisms underlying the association between mutant mtDNA and prostate cancer progression remain obscure. Mutant mtDNA is associated with increased genomic DNA double-strand breaks [7]. The resulting genomic instability could account for the multiple phenotypic effects observed in prostate cells harboring mutations/depletion of mtDNA, i.e. increased migration, acquisition of androgen-independence and progression to an invasive phenotype that is resistant to conventional chemotherapies [4-6]. We have identified the presence of large mtDNA deletions in prostate cancer specimens but not in age-matched benign prostate hyperplasia, and we have correlated their presence with loss of BRCA2 protein in prostate cancer. *BRCA2* is a known gene involved in repair of DNA double-strand breaks, and its loss confers a significantly elevated risk to develop aggressive, rapidly progressing, high-grade prostate carcinoma [8-9]. Down-regulation of BRCA2 expression in mtDNA-mutated cells occurs through a calcium-dependent activation of retrograde (mitochondria-to-nucleus) signaling leading to increased expression levels of two negative regulators of BRCA2 expression, i.e. Skp-2 and miRNA-1245 [10]. In turn, reduced BRCA2 protein in mtDNA-depleted cells results in increased sensitivity to PARP inhibitors, a novel class of anticancer drugs [10]. The outcome of this project has provided an understanding of the role of mutant mtDNA in prostate cancer progression, uncovering a novel mechanism by which mtDNA depletion restrains homologous recombination, and highlighting the role of mutations in mtDNA in modulating sensitivity to PARP inhibitors in transformed prostate cells.

BODY

Aim 1. Investigate the association between mutations in mtDNA and loss of BRCA2 protein in prostate cancer specimens *in vivo*

In this project we have demonstrated that the protein BRCA2 is reduced in prostate cancer specimens and high-grade prostatic intraepithelial neoplasia (Figure 1) and we have identified the presence of mtDNA large deletions in prostate cancer but not in age-matched benign prostate hyperplasia (Figure 2). We have also shown that the number of mtDNA deletions is associated with loss of BRCA2 protein levels in sporadic prostate carcinomas. No significant correlation was found between loss of BRCA2 protein and presence of mtDNA point mutations (Table 1). These data indicate that large mitochondrial genetic damage accompanies prostate malignant transformation and that it

may suppress the expression of the tumor suppressor BRCA2, a critical player of repair of DNA double strand breaks by homologous recombination.

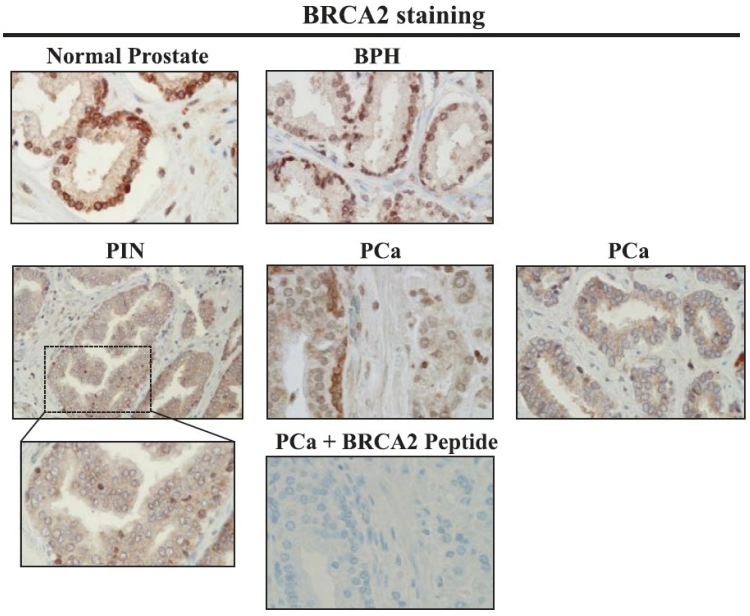

Figure 1. BRCA2 protein is lost in high-grade prostatic intraepithelial neoplasia (PIN) and in prostate adenocarcinomas. Prostate tissue macroarrays sections were stained using anti-BRCA2 antibody. Top: Nuclear and cytoplasmic BRCA2 localization in normal prostate and BPH (x400). Bottom: Significant loss of nuclear BRCA2 in high-grade PIN and prostae carcinomas (PCa). Two different PCa samples are shown (x400). Cytoplasmic and nuclear localization of BRCA2 in prostate carcinoma was suppressed by preincubation of the antibody with a competing peptide.

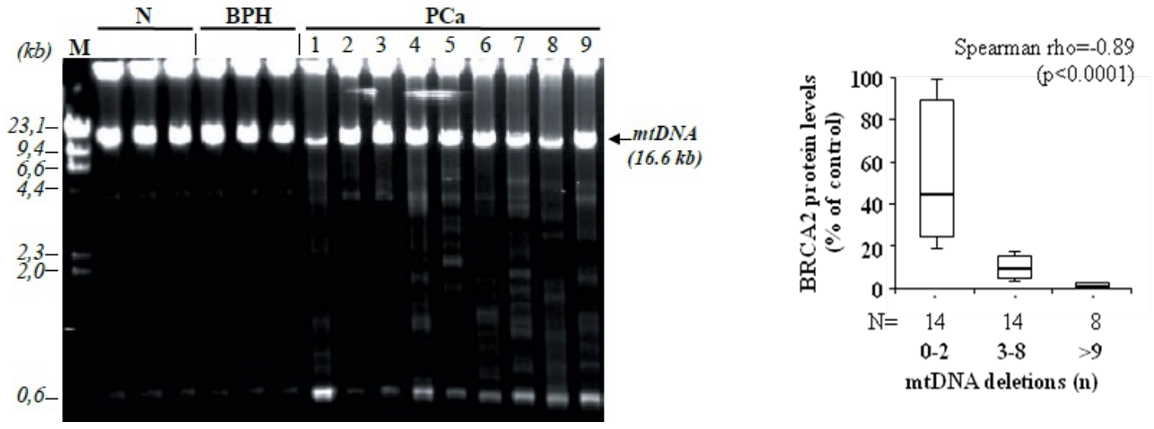

Figure 2. MtDNA large deletions are associated with reduced BRCA2 protein in human prostate carcinoma. (Left) Total DNA extracted from normal prostate (N; n=3), BPH (n=3) and prostate carcinoma (PCa; n=9) specimens was subjected to long-PCR analysis of the complete mtDNA. M= *molecular weight marker*. (Right) BRCA2 protein levels were negatively correlated

with the number of mtDNA deletions in prostate cancer specimens ($P < 0.0001$, Spearman's correlation coefficient testing).

Table 1. mtDNA point mutations, mtDNA large deletions and BRCA2 protein levels in prostate carcinoma specimens

	Point mutations										
Sample	*Base change*	*Amino-acid change*	*Gene*	*Het*	*PSIC*	*Somatic*	*Variability*	*ID*	*Large deletions (n)*	*mtDNA content (%)*	*BRCA2 protein (%)*
BPH 1	A15929G	—	*MT-TT*	–		n.a.	0.002	PA_XX_XX_183	0	83	45
BPH 2	T12713C	I126T	*MT-ND5*	–	0.003	n.a.	0.000	PA_XX_XX_188	2	98	61
BPH 3	G9300A	A32T	*MT-COIII*	–	0.000	n.a.	0.019	PA_XX_XX_184	0	100	62
BPH 4	T14501C	I58T	*MT-ND6*	–	0.514	n.a.	0.000	PA_XX_XX_185	0	98	89
BPH 5	A12634G	I100V	*MT-ND5*	–	0.925	n.a.	0.010	PA_XX_XX_186	1	100	84
	A13630G	T432A	*MT-ND5*	–	0.527	n.a.	0.006				
	T8668C	W48R	*MT-ATP6*	–	0.999	n.a.	0.004				
BPH 6	T5160C	S231P	*MT-ND2*	–	0.986	n.a.	0.000	PA_XX_XX_187	2	91	100
PCa 1	None							PA_XX_XX_168	7	34	5
PCa 2	T11204C	F149L	*MTND4*	–	0.000	Y	0.020	PA_XX_XX_169	6	98	5
PCa 3	None							PA_XX_XX_170	5	56	13
PCa 4	None							PA_XX_XX_171	5	89	11
PCa 5	C9739T	A178V	*MTCOIII*	–	0.018	N	0.000	PA_XX_XX_172	5	76	16
PCa 6	T11253C	I165T	*MTND4*	–	0.001	N	0.021	PA_XX_XX_173	6	98	16
PCa 7	G15428A	D228N	*MTCYTB*	+	0.999	Y	0.000	PA_XX_XX_174	13	100	8
	T12631G	S99A	*MTND5*	–	0.003	N	0.001				
PCa 8	None							PA_XX_XX_175	9	39	0.5
PCa 9	None							PA_XX_XX_176	10	79	0.5
PCa 10	None							PA_XX_XX_177	11	82	0.5
PCa 11	None							PA_XX_XX_178	13	60	0.5
PCa 12	G9738A	A178T	*MTCOIII*	–	0.219	N	0.007	PA_XX_XX_179	14	65	0.5
PCa 13	None							PA_XX_XX_180	7	81	7
PCa 14	A14220C	L152P	*MTND6*	–	0.999	N	0.000	PA_XX_XX_181	9	80	10
	G5849A	—	*MT-TY*	+		N	0.000				
PCa 15	None							PA_XX_XX_182	16	31	0.25

Abbreviations: BPH, benign prostate hyperplasia; Het, heteroplasmy; n.a., information not available; PCa, prostate carcinoma.

Aim 2. Identify the molecular mechanisms of down-regulation of BRCA2 expression by mutant mtDNA

By using prostate epithelial cells chemically depleted of their mtDNA pool, we have demonstrated that mtDNA depletion, a condition that resembles mtDNA large deletions, activates a calcium-dependent signaling pathway that induces up-regulation of the mRNA levels of Skp2, an ubiquitin ligase whose expression is associated with reduced levels of BRCA2, and of miRNA-1245, a negative regulator of BRCA2 expression at the translational level (Figure 3) [10]. BRCA1, another tumor suppressor known regulator of genome stability and homologous recombination, is not affected by mtDNA depletion [10]. Besides prostate cancer cells, we report that this mechanism occurs in other cancer cell types as well, including breast cancer [10].

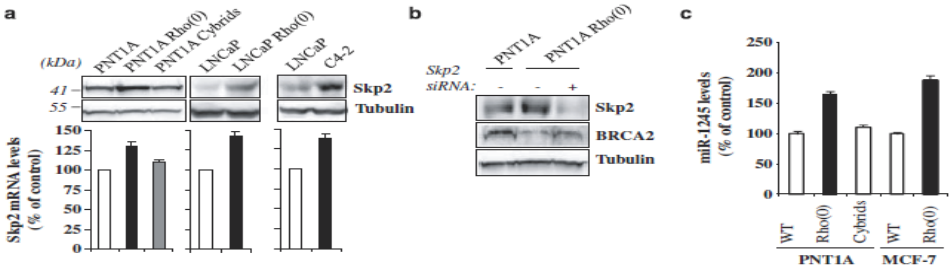

Figure 3. MtDNA depletion increases Skp2 protein and miR-1245 levels. (a) Skp2 protein and mRNA levels were analyzed in wild-type and mtDNA-depleted [Rho(0)] cells by Western blotting and real-time RT-PCR, respectively. (b) Wild-type and Rho(0) cells were transiently transfected with Skp2 siRNA or non-specific siRNA (-) and, after 48 h, analyzed for Skp2 and BRCA2 protein levels by Western blotting. (c) miR-1245 levels were monitored in wild-type (WT) and Rho(0) cells by real-time RT-PCR and expressed as percentage of wild-type cells. PNT1A, normal prostate epithelial cells; MCF-7, breast tumor cells; LNCaP, androgen-dependent prostate cancer cells; C4-2, androgen-independent prostate cancer cells.

Aim 3. Investigate the role of BRCA2 in preventing/hindering mtDNA-related prostate cancer progression

We report that loss of BRCA2 in mtDNA-depleted [Rho(0)] cells results in increased DNA double-strand breaks and impaired DNA damage response by homologous recombination. In turn, this phenotype promotes increased cell sensitivity to PARP inhibitors (Figure 4). Reconstitution of the mtDNA pool to wild-type levels (cybrid cells) restores sensitivity to the PARP inhibitor AG014699 to wild-type values (Figure 4).

PARP inhibitors have emerged as a novel class of anticancer drugs that function through a mechanism known as synthetic lethality, whereby two defective genes or pathways with negligible effect on cell viability turn lethal when combined in the same cell [11]. PARP-1 and -2 have an important role in signaling single-strand breaks (SSB) [12] and their inhibition results in accumulation of double-strand breaks (DSBs) and apoptosis unless rescued by upstream homologous recombination [12-13]. Effective HR depends upon BRCA1 and BRCA2, whose major function is to complex with Rad51 to orchestrate DNA repair. Tumors derived from patients with inherited mutations in BRCA1 or BRCA2 lack BRCA1 or BRCA2 activity and thus, upstream inhibition of PARP results in cancer cell apoptosis. Indeed, cells that are deficient in BRCA1 or BRCA2 are about 1000-fold more sensitive to PARP inhibitors than wild-type cells [14]. This model of synthetic lethality by PARP inhibitors is being proven effective in clinical trials for treatment of cancers having inherited mutations in *BRCA1* or *BRCA2* [15-16]. However, the potential value of these novel drugs in sporadic cancers has not yet been studied. We report that mtDNA depletion or large deletions might cooperate with PARP inhibition to induce cell death in cancer cells. We suggest that sporadic tumors harboring decreased BRCA2 protein resulting from mtDNA mutations may be responsive to PARP inhibitors.

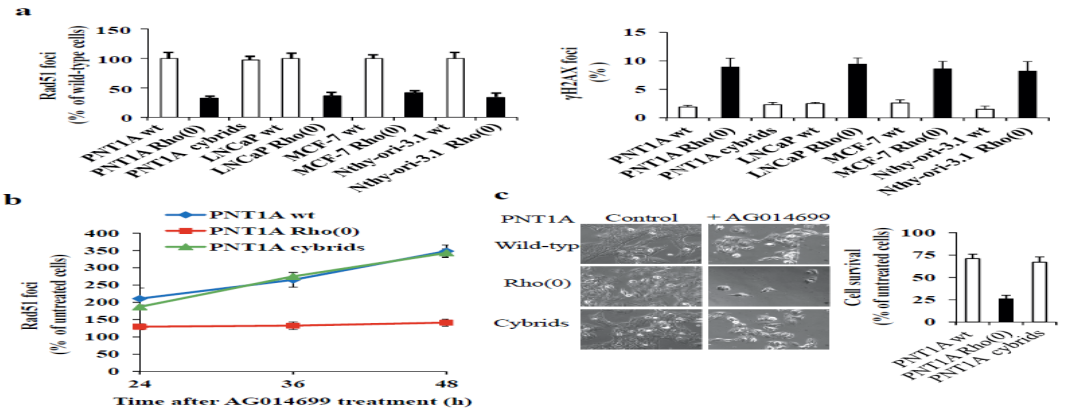

Figure 4. MtDNA depletion decreases HR and sensitizes cells to AG014699. (a) Wild-type (wt), cybrids and Rho(0) cells were analyzed for spontaneous double-strand breaks formation and repair by γH2AX and Rad51 immunofluorescence, respectively. The number of Rad51 foci was expressed as percentage of wild-type cells. (b-c) Cells were treated with 10 μM AG014699, a PARP inhibitor, or solvent up to 48 h, before incubation with fluorescently-labeled antibodies against Rad51 for double-strand breaks undergoing repair. (c) Wild-type and mtDNA-mutant cells treated with 10 μM AG014699 for 24 h were cultured in drug-free medium for 21 days, fixed, and counted. Cell survival was calculated as percentage of untreated controls. A representative experiment after 21 days is shown for PNT1A prostate cells.

KEY RESEARCH ACCOMPLISHMENT

- Characterize the expression of the tumor suppressor BRCA2 at various stages of prostate malignant transformation.

- Profile the spectrum of mtDNA alterations (large deletions, mtDNA point mutations, mtDNA content) in normal and cancer prostate tissues.

- Delineate the correlation between mtDNA mutations and reduced BRCA2 protein levels in prostate cancer specimens.

- Determine the retrograde signaling pathway responsible for mitochondrial DNA-dependent down-regulation of BRCA2 protein levels.

- Characterize the role of BRCA2 in the cellular response to pro-apoptotic drugs of mtDNA-depleted cells.

- Unveil the effect of mtDNA deletion in prostate cancer on degrading a tumor suppressor gene involved in the metastasis.

REPORTABLE OUTCOMES

FULL-LENGTH PAPERS

Tsai, Y.S., Chang, K-H., Wu, K., Tseng, S-F., Xie, D., Lai, C-H., Fazli, L., Gleave, M., Sun, H., Xiao, G., Gandee, L., Sharifi, N., Moro, L., Tzai1, T-S., Jer-Tsong Hsieh, J.T. (2014) The role of homeostatic regulation between tumor suppressor DAB2IP and oncogenic Skp2 in prostate tumorigenesis. Oncotarget (In press).

Arbini AA, Guerra F, Greco M, Marra E, Gandee L, Xiao G, Lotan Y, Gasparre G, Hsieh JT, Moro L. (2013) Mitochondrial DNA depletion sensitizes cancer cells to PARP inhibitors by translational and post-translational repression of BRCA2. *Oncogenesis* 2: e82.

Arbini AA, Greco M, Yao JL, Bourne P, Marra E, Hsieh JT, di Sant'agnese PA, Moro L. (2011) Skp2 Overexpression Is Associated with Loss of BRCA2 Protein in Human Prostate Cancer. *Amer J Pathol* 178: 2367-2376.

CONCLUSIONS

Mitochondrial DNA alterations, including large deletions, pathogenic point mutations and changes in mtDNA content, are observed virtually in any kind of tumor type, but their role in malignant transformation is still not completely understood. Several evidences have demonstrated that mtDNA depletion and pathogenic point mutations promote genome instability and confer an invasive phenotype, associated with increased

expression of pro-invasive genes [4-6, 17-18]. We provide new evidences on the pathogenic role of mutant mtDNA in prostate cancer etiology and have given a novel picture of the molecular players in the oncogenic pathway/s activated by mutant mtDNA, including Skp-2 and miR-1245, which could result in degrading potent tumor suppressor protein. Overall data provid new insights into prostate cancer molecular pathogenesis. In addition, we propose that mtDNA-mutated prostate tumors may be sensitive to PARP inhibitor chemotherapy owing their defects in homologous recombination.

REFERENCES

[1] Higuchi M. Roles of Mitochondrial DNA Changes on Cancer Initiation and Progression. Cell Biol (Henderson, NV) 2012;1.

[2] Desler C, Marcker ML, Singh KK, Rasmussen LJ. The importance of mitochondrial DNA in aging and cancer. J Aging Res 2011;2011:407536.

[3] Koochekpour S, Marlowe T, Singh KK, Attwood K, Chandra D. Reduced mitochondrial DNA content associates with poor prognosis of prostate cancer in African American men. PLoS One 2013;8:e74688.

[4] Higuchi M, Kudo T, Suzuki S, Evans TT, Sasaki R, Wada Y, et al. Mitochondrial DNA determines androgen dependence in prostate cancer cell lines. Oncogene 2006;25:1437-45.

[5] Moro L, Arbini AA, Marra E, Greco M. Mitochondrial DNA depletion reduces PARP-1 levels and promotes progression of the neoplastic phenotype in prostate carcinoma. Cell Oncol 2008;30:307-22.

[6] Moro L, Arbini AA, Yao JL, di Sant'Agnese PA, Marra E, Greco M. Mitochondrial DNA depletion in prostate epithelial cells promotes anoikis resistance and invasion through activation of PI3K/Akt2. Cell Death Differ 2009;16:571-83.

[7] Singh KK, Kulawiec M, Still I, Desouki MM, Geradts J, Matsui S. Inter-genomic cross talk between mitochondria and the nucleus plays an important role in tumorigenesis. Gene 2005;354:140-6.

[8] Castro E, Goh C, Olmos D, Saunders E, Leongamornlert D, Tymrakiewicz M, et al. Germline BRCA mutations are associated with higher risk of nodal involvement, distant metastasis, and poor survival outcomes in prostate cancer. J Clin Oncol 2013;31:1748-57.

[9] Castro E, Goh CL, Eeles RA. Prostate cancer screening in BRCA and Lynch syndrome mutation carriers. Am Soc Clin Oncol Educ Book 2013.

[10] Arbini AA, Guerra F, Greco M, Marra E, Gandee L, Xiao G, et al. Mitochondrial DNA depletion sensitizes cancer cells to PARP inhibitors by translational and post-translational repression of BRCA2. Oncogenesis 2013;2:e82.

[11] Kaelin WG, Jr. The concept of synthetic lethality in the context of anticancer therapy. Nat Rev Cancer 2005;5:689-98.

[12] Dantzer F, de La Rubia G, Menissier-De Murcia J, Hostomsky Z, de Murcia G, Schreiber V. Base excision repair is impaired in mammalian cells lacking Poly(ADP-ribose) polymerase-1. Biochemistry 2000;39:7559-69.

[13] Schultz N, Lopez E, Saleh-Gohari N, Helleday T. Poly(ADP-ribose) polymerase (PARP-1) has a controlling role in homologous recombination. Nucleic Acids Res 2003;31:4959-64.
[14] Farmer H, McCabe N, Lord CJ, Tutt AN, Johnson DA, Richardson TB, et al. Targeting the DNA repair defect in BRCA mutant cells as a therapeutic strategy. Nature 2005;434:917-21.
[15] Audeh MW, Carmichael J, Penson RT, Friedlander M, Powell B, Bell-McGuinn KM, et al. Oral poly(ADP-ribose) polymerase inhibitor olaparib in patients with BRCA1 or BRCA2 mutations and recurrent ovarian cancer: a proof-of-concept trial. Lancet 2010;376:245-51.
[16] Tutt A, Robson M, Garber JE, Domchek SM, Audeh MW, Weitzel JN, et al. Oral poly(ADP-ribose) polymerase inhibitor olaparib in patients with BRCA1 or BRCA2 mutations and advanced breast cancer: a proof-of-concept trial. Lancet 2010;376:235-44.
[17] Amuthan G, Biswas G, Zhang SY, Klein-Szanto A, Vijayasarathy C, Avadhani NG. Mitochondria-to-nucleus stress signaling induces phenotypic changes, tumor progression and cell invasion. EMBO J 2001;20:1910-20.
[18] Guha M, Avadhani NG. Mitochondrial retrograde signaling at the crossroads of tumor bioenergetics, genetics and epigenetics. Mitochondrion 2013;13:577-91.

APPENDIX

Tsai, Y.S., Chang, K-H., Wu, K., Tseng, S-F., Xie, D., Lai, C-H., Fazli, L., Gleave, M., Sun, H., Xiao, G., Gandee, L., Sharifi, N., Moro, L., Tzai1, T-S., Jer-Tsong Hsieh, J.T. (2014) The role of homeostatic regulation between tumor suppressor DAB2IP and oncogenic Skp2 in prostate tumorigenesis. Oncotarget (In press)

The role of homeostatic regulation between tumor suppressor DAB2IP and oncogenic Skp2 in prostate cancer growth

Yuh-Shyan Tsai[1,2], Chen-Li Lai[1], Chih-Ho Lai[3],Kai-Hsiung Chang[4],Kaijie Wu[5], Shu-Fen Tseng[6], Ladan Fazli[7], Martin Gleave[7],Guanghua Xiao[8], Leah Gandee[2], Nima Sharifi[4], Loredana Moro[9],Tzong-Shin Tzai[1*], Jer-Tsong Hsieh[2,10*]

Department of [1]Urology, Medical College and Hospital, National Cheng Kung University, Tainan 70401, Taiwan

Department of [2]Urology, and [8]Clinical Sciences, University of Texas Southwestern Medical Center, Dallas, TX75390, USA

School of [3]Medicine and Graduate Institute of Basic Medical Science, China Medical University, Taichung 404, Taiwan

Department of [4]Cancer Biology, Lerner Research Institute, Cleveland Clinic, Cleveland, OH 44195, USA

Department of [5]Urology, The First Affiliated Hospital, Medical School of Xi'an Jiaotong University, Xi'an 710061, China

Department of [6]Bioengineering, University of Texas at Arlington, Arlington, TX76019, USA

[7]VancouverProstate Center, University of British Columbia, Vancouver, British Columbia V6K 2P5, Canada

[9]Institute of Biomembranes and Bioenergetics, National Research Council (C.N.R.), Bari, Italy

[10]Graduate Institute of Cancer Biology, China Medical University, Taichung 404, Taiwan

***Correspondence:**

Jer-Tsong Hsieh, Department of Urology, University of Texas Southwestern Medical Center, 5323, Harry Hines Blvd., Dallas, TX75390-9110, Fax: 214-648-8786, E-mail: JT.Hsieh@UTSouthwestern.edu

Tzong-Shin Tzai, Department of Urology, Medical College and Hospital, National Cheng Kung University, Tainan 70401, Taiwan.E-mail: tts777@mail.ncku.edu.tw

Running title: Reciprocal interaction between Skp2 and DAB2IP

Key words: prostate neoplasm, Skp2, DAB2IP, ubiquitin

Declaration of interest

The authors declare that there is no conflict of interest.

Financial support

This work was supported by United States Army Grant W81XWH-10-1-0176 to JTH and NSC Grant (98-2314-B-006-033-MY2) from Taiwan. Dr. Yuh-Shyan Tsai was supported by a fellowship from National Cheng Kung University Hospital, Tainan, Taiwan.

Abstract

Altered DAB2IP gene expression often detected in prostate cancer (PCa) is due to epigenetic silencing. In this study, we unveil a new mechanism leading to the loss of DAB2IP protein; an oncogenic S-phase kinase-associated protein-2 (Skp2) as E3 ubiquitin ligase plays a key regulator in DAB2IP degradation. In order to unveil the role of Skp2 in the turnover of DAB2IP protein, both prostate cell lines and prostate cancer specimens with a variety of molecular and cell biologic techniques were employed. We demonstrated that DAB2IP is regulated by Skp2-mediated proteasome degradation in the prostate cell lines. Further analyses identified the N-terminal DAB2IP containing the ubiquitination site. Immunohistochemical study exhibited an inverse correlation between DAB2IP and Skp2 protein expression in the prostate cancer tissue microarray. In contrast, DAB2IP can suppressSkp2 protein expression is mediated through Akt signaling. The reciprocal regulation between DAB2IP and Skp2 can impact on the growth of PCa cells. This reciprocal regulation between DAB2IP and Skp2 protein represents a unique homeostatic balance between tumor suppressor and oncoprotein in normal prostate epithelia, which is apparently altered in cancer cells. The outcome of this study has identified new potential targets for developing new therapeutic strategy for PCa.

Introduction

Prostate cancer continues as the leading male malignancy with significant mortality in the United States [1]; for example, an estimated 233,000 new cases and 29,480 deaths in 2014 [1]. Several unique genetic events were reported to be associated with the development of prostate cancer, including NKX3.1 inactivation, TMPRSS2-ERG fusion, MYC amplification, PTEN mutation, and EZH2 overexpression [2]. In addition to genetic event, our data indicate that DAB2IP, a novel family of RasGTPase-activating protein family as a potent tumor suppressor, is epigenetically silenced [3, 4], which is suppressed by EZH2 and other epigenetic machinery such as DNA methylation and histone acetylation [5-7]. DAB2IP plays an important role in regulating the cell growth and survival of prostate cancer [4] through its GAP domain in suppressing Ras-Raf-ERK activation or proline-rich (PR) domain in suppressing PI3K-dependent Akt phosphorylation. Also, DAB2IP can elicit cell apoptosis via apoptosis-stimulated kinase (ASK1)-JNK pathway [8]. Furthermore, DAB2IP can prevent the progression of prostate cancer [5, 9] by inhibiting epithelial-to-mesenchymal transition (EMT) via Wnt-elicited β-catenin pathway. S-phase-associated kinase protein-2 (Skp2) is a member of Skp, Cullin, F-box containing complex [10] that functions as an ubiquitin E3 ligase, which is significantly elevated in prostate cancer. A genomic analysis reported increased copy number of *Skp2* gene in advanced metastatic prostate cancer [11]. Skp2 can regulate several cellular functions responsible for prostate cancer progression, including cell cycle progress, signal transduction, or DNA repair [12]. Noticeably, these substrates includes p27 [13], p21 [14], BRCA2 [15], smad4 [16], and Myc [17]. On the other hand, several factors can influence Skp2 activity, stability, and subcellular translocation. Akt appears to a key factor to phosphorylate Skp2 and cause activated Skp2 translocation into cytoplasm, which also prevents Skp2 from degrading by anaphase-promoting complex/cyclosome-Cdh1 (APC/C-Cdh1) complex [18, 19]. It is known that Skp2 can be regulated by Wnt-signaling pathway in human invasive urothelial cancer cells through the binding of TCF4 and β-catenin to its promoter [20] or through NF-κB, p53 and Akt/GSK-3β pathway [21]. However, the regulation of Skp2 in prostate epithelia remained largely unknown. Therefore, these findings prompt us to explore the relationship between DAB2IP and Skp2 in human prostate epithelial and cancer cells.

Results

Skp2-mediated ubiquitin-proteasome system (UPS) regulates post-translational expression of DAB2IP

We noticed that there is an inverse correlation between DAB2IP and Skp2 protein expression (Fig. 1A) in an immortalized normal prostate cell line (PNT1A) and its derivative PNT1A ρ(0), a mitochondrial DNA-deficient cell with neoplastic phenotypes [22]. Noticeably, DAB2IP protein levels in cybrids [22], derived from PNT1A ρ(0) after restoring mitochondrial DNA by fusing with platelets, were similar to those in PNT1A cells (Fig. 1A). No difference of DAB2IP mRNA levels in these cells was detected (Fig. 1A, lower panel), which rules out the transcriptional regulation. A similar expressions pattern of DAB2IP protein was also observed in another immortalized normal prostate cell line (PZ-HPV-7) and its tumorigenic subline (PZ-HPV-7T) [23] (Fig. 1B). By manipulating Skp2 expression level using cDNA or shRNA transfection in PC3, PNT1A, PZ-HPV-7T and 293J cells, the inverse correlation of DAB2IP and Skp2 protein expression was observed (Fig. 1C-F). We therefore decided to determine the impact of UPS on DAB2IP protein turnover. In the presence of proteasome inhibitor (MG132), DAB2IP protein elevated in PTN1A ρ(0) cells in a time-dependent manner (Fig. 2A). Using IP, we found that ubiquitinated DAB2IP form a complex with Skp2 and accumulated total and ubiquitinated DAB2IP was observed in MG132-treated PTN1A ρ(0) cells (Fig. 2B). Similarly, MG132 treatment resulted in the elevation of DAB2IP in PZ-HPV-7T cells (Fig. 2C). Also, ectopic ubiquitin expression resulted in increasing ubiquitinated DAB2IP but decreasing DAB2IP level in a dose-dependent manner (Fig. 2D). In PC3 cells, both elevated DAB2IP protein levels and DAB2IP-Skp2 complex were detected after treating with MG132 (Fig. 2E). Also, in 293J cells transiently transfected with DAB2IP expression vector, DAB2IP protein formed a complex with endogenous Skp2 in a dose-dependent manner (Fig. 2F). In addition, knocking down the endogenous Skp2 resulted in an elevation of DAB2IP protein and a reduction of ubiquitinatedDAB2IP in a dose-dependent manner (Fig. 2G). Using constitutively active Skp2 [18, 19], reduced DAB2IP protein was detected in 293 wild-type (wt) cells (Fig.2H), Taken together, Skp2-mediated UPS plays an important role in regulating DAB2IP protein expression post-translationally in both immortalized normal prostate epithelial and cancer cells.

N-terminal DAB2IP contains ubiquitinationsites

To map the ubiquitination site of DAB2IP protein, plasmids containing His-tagged Skp2 gene and different constructs of DAB2IP cDNA (Fig. 3A) were co-transfected into 293wt cells. Subsequently, His-tagged proteins were affinity-purified and

analyzed by immunoblotting. Results (Fig. 3B) showed that both full-length and N-terminal DAB2IP protein could be ubiquitinated and form complexes with Skp2. Although Skp2 can bind to C-terminal DAB2IP, there is no ubiquitination site (Fig. 3B). Using different domains of N-terminal DAB2IPcDNA, data from *in vivo* ubiquitination assay further indicated that GAP, C2 and PHC2 domains, but not PH domain alone can be ubiquitinated and degraded (Fig. 3C). Similar findings were shown in the *in vivo* ubiquitination assay for FΔPH, FΔLZ, and GAPC fragments (Fig. S1). Furthermore, according to the predicted ubiquitination sites (http://ubpred.org/index.html) for N-terminalDAB2IP, there are three potential ubiquitination sites in GAP domain including K246, K248 and K334. Using site-directed mutagenesis, we found that the mutant containing all three sites significantly reduced DAB2IP ubiquitination (Fig. 3D).

DAB2IP regulates Skp2 degradation through Akt signaling

We noticed that DAB2IP was able to suppress Skp2 expression in 293J cells (Fig. 2F and 4A). Elevated expression of DAB2IP resulted in a reduction of Skp2 expression and an accumulation of ubiquitinated Skp2 in 293J cells (Fig. 4B). Further investigation in 293wt (Fig. 4C) showed that increased DAB2IP expression was able to decrease Skp2 protein levels and this reduction could be reversed in the presence of continuously active Akt (Akt-CA).

Moreover, by knocking down DAB2IP (KD), both LAPC4 and PZ-HPV-7 cells [24] exhibited increasing expression of Skp2 and phosphorylated Akt (pAkt) compared with the control cells (Con), the decreased p27 protein level revealed the degradation activity of Skp2 for its substrate (Fig. 4D). Increased Skp2 protein did not correlate with *Skp2* mRNA levels in DAB2IP KD cells (Fig. 4D), suggesting that the regulation of Skp2 protein is mediated by Akt at post-transcriptional level. Thus, we determined the half-life of Skp2 and the results showed that the half-life of Skp2 is longer in PZ-HPV-7 KD than its control cell (Fig. 4E). And also, in the presence of pAkt inhibitor LY294002 (10 μM), the half-life of Skp2 protein reduced significantly (Fig. 4F). Our results indicate that DAB2IP is able to facilitate Skp2 degradation by inhibiting Akt activity.

The reciprocal regulation between DAB2IP and Skp2 is involved in the growth of prostatic epithelia both *in vitro* and *in vivo*

To evaluate the impact of interaction between DAB2IP and Skp2 on cell growth, MTT assay and soft agar colony formation assay (CFA) were carried out by using immortalized normal prostate cell, PZ-HPV-7. As shown in Fig. 5A and B, PZ-HPV-7 KD cells displayed higher growth rate and numbers of cells formed in the colonies

accompanied with increased expression of Skp2 protein levels. Knocking down Skp2 expression using transient transfection of Skp2 shRNA reversed the growth rate of PZ-HPV-7 KD cells (Fig. 5A). In addition, cells were implanted subcutaneously into nude mice and the potential of tumor growth of the cells were evaluated. DAB2IP KD cells formed tumors in 100 % [18] of the experimental mice in an *in vivo* xenograft model (Fig. 5C). In general, PZ-HPV-7 KD acquired *in vitro* growth rate, anchorage independent growth, and *in vivo* tumorigenic potential. Reverse of cell growth rate by repressing Skp2 expression in PZ-HPV-7 KD suggests a regulatory role of the interaction between DAB2IP and Skp2 in cell proliferation. We further determined whether there is a similar role of interaction between DAB2IP and Skp2 in PCa cells. C4-2 cell line, an androgen-independent line derived from androgen-sensitive LNCaP [25], showed higher Skp2 expression and lower DAB2IP expression than LNCaP cells (Fig 5D). Knocking down the endogenous Skp2 in C4-2 cells resulted in an elevation of DAB2IP level accompanied with growth inhibition (Fig. 5D, E), in which the change of DAB2IP mRNA levels was not significant (Fig. 5D, right panel). Furthermore, knocking down DAB2IP mRNA in C4-2-Skp2 shRNA cells did restore the growth rate (Fig. 5E). Altogether, our data indicate that the Skp2- DAB2IP interaction can impact on PCa cell growth.

The expressions of DAB2IP and Skp2 in human PCa specimens

Owing to the inverse correlation of DAB2IP and Skp2 proteins, which was not due to transcriptional regulation, observed in cell lines, we would like to find out whether the phenomenon can be seen in clinical specimens. We explored three different datasets of cDNA arrays (GSE21034, GSE6099, and GSE17951) of human prostate cancer patients to see whether similar feature can be found. The correlation co-efficiencies were -0.21, 0.001, and -0.10, respectively. Only GSE21034 dataset showed a significantly inverse relationship between *DAB2IP* and *Skp2* mRNA expression (p = 0.014). Overall, there was no significant correlation between DAB2IP and Skp2 using a meta-analysis method (chi-square =10.49, DF=3, p = 0.105) (Fig. 6A). Additionally, we probed both DAB2IP and Skp2 proteins in two tissue microarrays containing 263 PCa specimens using immunohistochemical staining (IHC). Among them, 69 (26.2%) or 37 (14.1%) PCa specimens exhibited $DAB2IP^{high}$ -$Skp2^{low}$ or $DAB2IP^{low}$-$Skp2^{high}$ pattern, respectively (Fig. 6B). Although statistically there is no correlation between the expressions of these two proteins in PCa specimens, an inverse correlation was still observed in approximate 40% of the PCa specimens.

Discussion

DAB2IP is known as a tumor suppressor in several cancers, such as breast, lung and hepatocellular carcinoma [26-28]). In addition, genome-wide association studies also indicate that single nucleotide polymorphism of DAB2IP gene is associated with not only the risk of aggressive PCa and other non-malignant diseases such as abdominal aortal aneurysm and cardiovascular diseases [29, 30]. In general, loss of DAB2IP in cancer cells is due to its epigenetic silencing [5, 6, 26-28]. However, in this study, we unveil additional mechanism leading to the loss of DAB2IP protein that is regulated by Skp2-mediated UPS. Interestingly, DAB2IP is also able to regulate Skp2 protein stability through Akt-mediated pathway [18, 31]. Most importantly, the reciprocal regulation between these two proteins plays an important role in influencing tumor behaviors of PCa.

In our results, although N- or C-terminal domain of DAB2IP protein can interact with Skp2, several potential ubiquitination sites are found in the C2 and GAP domain of the N-terminal. The lysine-rich clusters found in the C2 domain that can bind to Ask1, PP2A, and GSK-3βleading to enhance cell apoptosis or prevent epithelial-to-mesenchymal transition [8, 24, 32] appear not the ubiquitination sites for Skp2. In contrast, within the GAP domain, K246, K248 and K334 are key sites for Skp2-eliicted ubiquitination. On the other hand, Skp2 recognizes substrate(s) for ubiquitylation usually through the phosphorylated consensus sequence(s) rather than recognizing a degron [33-35]. For instance, the phosphorylated Thr187 of p27(Kip1) binds to Skp2 through Cks1-phosphate binding site [34]. Nevertheless, the consensus sequence for phosphorylation inSkp2 substrates and whether it is essential for initiating the ubiquitination are still not fully understood. Similarly, the requirement of DAB2IP phosphorylation in Skp2 recognition needs further study.

Interestingly, DAB2IP can also regulate Skp2 protein stability in normal or benign cells. It is known that the regulation of Skp2 degradation is complex and involves multiple mechanisms. Skp2 gene expression can be regulated by p53 and NF-κB through Akt-GSK-3β pathway [21]. Also, TCF4 and β-catenin can regulate Skp2 gene expression through the binding of TCF/LEF1 to Skp2 promoter [20]. Besides the regulation at gene expression level, Skp2 can be degraded via auto-ubiquitination in Cul1-dependent [36], or Cdh1 dependent manners. Also, p107 has been reported to promote Skp2 degradation independent of either Cul1 or Cdh1 [37]. In addition, Akt mediated phosphorylation stabilized Skp2 by evading from APC/Cdh1-mediated proteasomal degradation [31, 38]. Since DAB2IP can function as a signalosome platform for coordinating protein-protein interaction from various signaling pathways including Ask1-JNK [8, 32], PIK3-Akt [32], PP2A-β catenin [24], and NF-κB [5], it is likely that DAB2IP modulate Skp2 through these pathways, especially through

inhibiting Akt activity. However, we can't completely rule out any other pathways also involved in this regulation.

Several previous studies using PCa specimens clearly indicate the association of Skp2, as a potential oncoprotein, with disease progression. De Marzo *et al*. and Arbini *et al*. reported that nuclear staining of Skp2 in PCa specimens is associated with more aggressive behavior [39, 40] . Other studies indicated that the cytoplasmic Skp2 protein exhibits E3 ubiquitin ligase activity and correlates with disease progression [18, 19]. Drobnjak *et al* reported that Skp2 staining in African-American, a population known to have the highest risk and more aggressive type of this cancer, PCa specimens is mainly cytoplasmic [41]. Furthermore, the accumulation of cytoplasmic Skp2 due to Akt-elicited Skp2 phosphorylation at serine 72 was associated with tumor cells expressing elevated Akt or reduced PTEN [19, 31]. In this study, about 40% of the PCa specimens showed an inverse correlation either $DAB2IP^{low}/Skp2^{high}$ (14.1%) or $DAB2IP^{high}/Skp2^{low}$ (26.2%). Taken together, Skp2 is a potent oncoprotein in subset of PCa patients.

In summary, we demonstrated a reciprocal regulation between DAB2IP, a tumor suppressor, and Skp2, an oncogenic protein, in normal prostatic epithelia and PCa cells, which represents paradigm shift of signalosome pattern in normal cell to malignant tumor. Based on these findings, it provides new therapeutic strategy for targeting Skp2 as a targeted therapy in PCa patients.

Materials and Methods

Plasmid constructs

Various expression plasmids for DAB2IP: F-, C-, N-, PH, PHC2, KA1/2, FΔPH, FΔLZ and DAB2IP shRNA were described previously [8, 24, 42, 43]. Additional expression plasmids: C2, GAP, GAPC from N-DAB2IP; FΔPH from F-DAB2IP; 3 mutants from N-DAB2IP (i.e., K246R/K248R, K334R, and K246R/K248R/K334R) using site-directed mutagenesis kits (QuikChange®, Stratagene). Skp2shRNA (sc-36499-SH) and its control plasmid were purchased from Santa Cruz Biotechnology. Skp2 cDNA and its derivative mutants (S72A, S72D, S64A, S64D) were kindly gifted from Dr. Hui-Kuan Lin (MD Anderson Cancer Center, Houston, TX) [19]. The plasmids pcDNA3.1-ubiquitin, and pcDNA3.1- ubiquitin ISG15 were obtained from Dr. Dimitris Xirodimas (University of Dundee, Scotland, UK). The plasmid carrying Akt-CA cDNA was provided by Dr. David Boothman (UT Southwestern Medical Center, Dallas, TX).

Cell culture, Antibodies, Reagents, and plasmids transfection

PNT1A, PC3, LNCaP, PZ-HPV-7, C4-2, LAPC4, 293 and their sublines were maintained as described previously [22-24, 32]. Anti-DAB2IP polyclonal antibody was used for western blot analysis and IHC as described previously [24, 32]. Anti-FLAG-HRP (M2) was obtained from Sigma (St. Louis, MO). Anti-Skp2 (sc74477), anti-Ubiquitin (sc271289), anti-Tubulin (32239), anti-Akt 123 (H36, sc8312), and anti-GAPDH (sc16674) were purchased from Santa Cruz Biotechnology (Santa Cruz, CA). Anti-phospho-Akt (Ser473) polyclonal antibody (#9271) was from Cell signaling Technology (Danvers, MA). Anti-p21 (6B6) and Anti-p27 were obtained from BD Pharmingen (Sparks, MD). Anti-Skp2 (2C8D9) was from Zymed (South San Francisco, CA). Proteasome inhibitor MG132 was purchased from Calbiochem (Gibbstown, NJ), cycloheximide and 2-(4-morpholinyl)-8-phenyl-chromone (LY294002) were also purchased from Sigma. For cDNA transfection, cells were seeded in plates with 70-80% confluence before transfection. The transfection was carried out using Lipofectamine LTX with Plus™ reagent (Invitrogen, Carlsbad, CA) or polyethylenimine (PEI, Polysciences Inc., Warrington, PA) according to the manufacturer's instructions.

qRT-PCR analysis

The total RNA was extracted with RNeasy mini kit (Qiagen, Valencia, CA) treated with RNase-free DNase I (Qiagen) and subjected to a cDNA synthesis kit (Bio-Rad, Hercules CA).The cDNA was further amplified in a 25 ml quantitative PCR reaction mixture containing 12.5µg of iQ^{TM} SYBGREEN Supermix® (Bio-Rad) and the studied primers using an iCycleriQ machine (Bio-Rad). The sequences of primers forDAB2IP are 5'-TGGACGATGTGCTCTATGCC-3' (forward) and

5'-GGATGGTGATGGTTTGGTAG-3' (reverse). Primers for Skp2 are 5'-AGCCCGACAGTGAGAACATC-3' (forward) and 5'-GAAGGGAGTCCCATGAAACA -3' (reverse). Primers for 18S RNA are 5'-GGAATTGACGGAAGGGCACCACC-3' (forward) and 5'-GTGCAGCCCCGGACATCTAAGG-3' (reverse).The PCR amplification protocol was 95 °C (3 minutes), 36 cycles of amplification cycle (95 °C [30 second], 55 °C [30 second], and 72 °C [1 minute]). All the data were done in duplicates and were repeated at least twice. The relative level of *DAB2IP* or *Skp2* mRNA from each sample was calculated by normalizing with *18S*cDNA.

Western blot assay

For western blot analysis, cells were washed twice with cold PBS first and lysed in 1.5 mL of cold RIPA buffer [44]mixed with fresh complete protease inhibitor cocktail (Roche, Indianapolis, IN) for 20 minutes on ice. After sonication with a microtipped sonifier at setting 3 for 20 seconds to reduce viscosity and centrifugation, cell lysates were subjected to western blot analysis.

Immunoprecipitation (IP)

Cell lysates lysed with RIPA buffer were further subjected to IP. In brief, anti-Skp2, anti-ubiquitin, or their control antibodies were incubated with Dynabead (Invitrogen) first for 15 minutes at room temperature, and mixed with the indicated cell lysates for 45 minutes. The eluted fraction was further immunoblotted with DAB2IP, Skp2, or other antibodies indicated in each figure.

***In vivo* Ubiquitination assay**

This assay was modified from Treier et al [45] and McMahon et al [46]. The input fraction was prepared using RIPA buffer. His-tagged protein was pulled down using Dynabead® His-Tag Isolation & Pulldown (Invitrogen) or MagneHis™ Protein Purification System (Promega, Madison, WI). Briefly, HEK293 cells (1×10^6) seeded at a 10-cm dish were transfected with pcDNA3.1 His-Ubiquitin, or His-Skp2 vectors along with the indicated plasmids. Approximately 36 h after transfection, cells were treated with 10 μM MG132 for 6 hours. Then, cell pellets were harvested and equally aliquoted into three 1.5 cm eppendorf tubes for the input, pull-down, and backup. The backup tube was immediately stored at -80 ^{o}C freezer. The input fraction was prepared using the RIPA buffer described as above. His-tagged protein was pulled down using Dynabead® His-Tag Isolation & Pulldown (Invitrogen) or MagneHis™ Protein Purification System (Promega). Briefly, the cell suspension was lysed by adding 1.0 ml of buffer A (6 M guanidinium-HCI, 0.1 M Na_2HPO_4/NaH2PO_4 pH 8.0 supplemented with 5 mM imidazole). The cell lysate was mixed with 50 μl of His-Tag magnetic beads and sonicated, then the mixture was incubated at room temperature

for 2 hours and overnight at 4 °C. Thereafter, the beads were washed sequentially with buffer A supplemented with 10 mM 2-mercaptoethanol (2-ME), buffer B (8 M urea, 10 mMTris, 0.1 MNa_2HPO_4/NaH2PO_4, pH 8.0) supplemented with 10 mM 2-ME, buffer C (8 M urea, 10 mMTris, 0.1 M Na_2HPO_4/NaH2PO_4, pH 6.3) supplemented with 10 mM 2-ME and 0.2% (v/v) Triton X-100, and finally, buffer C supplemented with 10 mM 2-ME and 0.1% (v/v) Triton X-100. Bound material was eluted from the beads by suspension in 75 μL of modified Laemmli sample buffer (20 mMTris-Cl, pH 6.8, 10% [v/v] glycerol, 0.8% [w/v] SDS, 0.1% [w/v] bromphenol blue, 720 mM 2-ME, and 500 mM imidazole) followed by the incubation at 70^{o}C water bath for 10 minutes. The eluted samples were collected and referred to as the "pull-down" fraction. Both of the input and pull-down fraction were subjected to SDS-PAGE and western blot analyses.

MTT assay and Soft agar colony formation assay

For cell growth assay, 1×10^3 cells per well were seeded in 96-well plates for the indicated time. Cell growth rate was calculated using 3-(4,5-dimethylthiazol-2-yl)-2,5-diphenyltetrazolium bromide (MTT) assay (Roche). The relative cell number was calculated by normalizing with Day 1 (=1).

For soft agar colony formation assay, 1×10^3 cells/well were plated on agar in the 24-well plates according to Sato et al [47].Two weeks later, the plates were fixed with 4% paraformaldehyde and stained in crystal violet solution. The number of colony was counted.

Xenograft formation and Histology examination

PZ-HPV-7 KD and its control (1×10^6) cells were injected into nude mice subcutaneously. The tumor incidence was recorded every other day until 6 weeks after inoculation. All the tumors were excised for histological examination using H&E staining.

IHC Staining

Two serial sections of two tissue microarrays containing human prostate tumor tissues were subjected to Ventana autostainer model Discover XT ™ (Ventana Medical System, Tuscan, AZ). The primary antibodies were anti-DAB2IP [23, 24]and anti-Skp2 (2C8D9) from Zymed, San Francisco, CA. Two pathologists assessed and scored the immunostaining independently and reached a final consensus for any inconsistent scoring. Briefly, values on a four-point scale were assigned to each specimen. The intensity score was assigned, which represented the average intensity of positive cells (0, none; 1, weak or questionably present stain; 2, intermediate intensity in a minority of cells; and 3, strong intensity in a majority of cells). High expression was defined as score higher than average, and low expression was defined as score lower than average.

Immunofluorescence staining

293 cells were cultivated and transfected with plasmids containing full-length gene of DAB2IP. Cells were fixed with 4% paraformaldehyde 24 hours after transfection and penetrated with 0.5% Triton-X100. Five percent of goat serum was used as blocking reagent, and primary antibodies against DAB2IP or Skp2 were applied on cells. After an overnight incubation at 4 °C, cells were washed and subjected to secondary antibodies conjugated with Alexa Fluor. DAPI was used as nuclear counterstaining. Afterward, staining results were evaluated under fluorescence microscope or confocal microscope.

Microarray database analysis

Three microarray data sets of PCa were obtained from the NCBI Gene Expression Omnibus (GEO): GSE21034 (n = 218) [48], GSE6099 (n = 83) [49], and GSE17951 (n = 153) [50]. Using quantile normalization, the Spearman correlation coefficient was calculated between *DAB2IP, Skp2* and individual genes and ranked in individual data sets as described previously [51]. All data were analyzed by using GraphPad Prism 5 (GraphPad, Inc., La Jolla, CA) and SPSS13.0 software package (SPSS Inc., Chicago, IL). The $p<0.05$ was considered as significant.

Reference

1. Siegel R, Ward E, Brawley O and Jemal A. Cancer statistics, 2011: the impact of eliminating socioeconomic and racial disparities on premature cancer deaths. CA Cancer JClin. 2011; 61(4):212-236.
2. Shen MM and Abate-Shen C. Molecular genetics of prostate cancer: new prospects for old challenges. Genes Dev. 2010; 24(18):1967-2000.
3. Chen H, Pong RC, Wang Z and Hsieh JT. Differential regulation of the human gene DAB2IP in normal and malignant prostatic epithelia: cloning and characterization. Genomics. 2002; 79(4):573-581.
4. Wang Z, Tseng CP, Pong RC, Chen H, McConnell JD, Navone N and Hsieh JT. The mechanism of growth-inhibitory effect of DOC-2/DAB2 in prostate cancer. Characterization of a novel GTPase-activating protein associated with N-terminal domain of DOC-2/DAB2. JBiolChem. 2002; 277(15):12622-12631.
5. Min J, Zaslavsky A, Fedele G, McLaughlin SK, Reczek EE, De RT, Guney I, Strochlic DE, Macconaill LE, Beroukhim R, Bronson RT, Ryeom S, Hahn WC, Loda M and Cichowski K. An oncogene-tumor suppressor cascade drives metastatic prostate cancer by coordinately activating Ras and nuclear factor-kappaB. NatMed. 2010; 16(3):286-294.
6. Chen H, Tu SW and Hsieh JT. Down-regulation of human DAB2IP gene expression mediated by polycomb Ezh2 complex and histone deacetylase in prostate cancer. JBiolChem. 2005; 280(23):22437-22444.
7. Jeronimo C, Bastian PJ, Bjartell A, Carbone GM, Catto JW, Clark SJ, Henrique R, Nelson WG and Shariat SF. Epigenetics in prostate cancer: biologic and clinical relevance. EurUrol. 2011; 60(4):753-766.
8. Zhang R, He X, Liu W, Lu M, Hsieh JT and Min W. AIP1 mediates TNF-alpha-induced ASK1 activation by facilitating dissociation of ASK1 from its inhibitor 14-3-3. JClinInvest. 2003; 111(12):1933-1943.
9. Hsieh JT, Karam JA and Min W. Genetic and biologic evidence that implicates a gene in aggressive prostate cancer. JNatlCancer Inst. 2007; 99(24):1823-1824.
10. Schulman BA, Carrano AC, Jeffrey PD, Bowen Z, Kinnucan ER, Finnin MS, Elledge SJ, Harper JW, Pagano M and Pavletich NP. Insights into SCF ubiquitin ligases from the structure of the Skp1-Skp2 complex. Nature. 2000; 408(6810):381-386.
11. Robbins CM, Tembe WA, Baker A, Sinari S, Moses TY, Beckstrom-Sternberg S, Beckstrom-Sternberg J, Barrett M, Long J, Chinnaiyan A, Lowey J, Suh E, Pearson JV, Craig DW, Agus DB, Pienta KJ, et al. Copy number and targeted mutational analysis reveals novel somatic events in metastatic prostate tumors.

Genome Res. 2011; 21(1):47-55.
12. Frescas D and Pagano M. Deregulated proteolysis by the F-box proteins SKP2 and beta-TrCP: tipping the scales of cancer. NatRevCancer. 2008; 8(6):438-449.
13. Tsvetkov LM, Yeh KH, Lee SJ, Sun H and Zhang H. p27(Kip1) ubiquitination and degradation is regulated by the SCF(Skp2) complex through phosphorylated Thr187 in p27. CurrBiol. 1999; 9(12):661-664.
14. Yu ZK, Gervais JL and Zhang H. Human CUL-1 associates with the SKP1/SKP2 complex and regulates p21(CIP1/WAF1) and cyclin D proteins. ProcNatlAcadSciUSA. 1998; 95(19):11324-11329.
15. Moro L, Arbini AA, Marra E and Greco M. Up-regulation of Skp2 after prostate cancer cell adhesion to basement membranes results in BRCA2 degradation and cell proliferation. JBiolChem. 2006; 281(31):22100-22107.
16. Liang M, Liang YY, Wrighton K, Ungermannova D, Wang XP, Brunicardi FC, Liu X, Feng XH and Lin X. Ubiquitination and proteolysis of cancer-derived Smad4 mutants by SCFSkp2. MolCell Biol. 2004; 24(17):7524-7537.
17. Kim SY, Herbst A, Tworkowski KA, Salghetti SE and Tansey WP. Skp2 regulates Myc protein stability and activity. MolCell. 2003; 11(5):1177-1188.
18. Gao D, Inuzuka H, Tseng A, Chin RY, Toker A and Wei W. Phosphorylation by Akt1 promotes cytoplasmic localization of Skp2 and impairs APCCdh1-mediated Skp2 destruction. NatCell Biol. 2009; 11(4):397-408.
19. Lin HK, Wang G, Chen Z, Teruya-Feldstein J, Liu Y, Chan CH, Yang WL, Erdjument-Bromage H, Nakayama KI, Nimer S, Tempst P and Pandolfi PP. Phosphorylation-dependent regulation of cytosolic localization and oncogenic function of Skp2 by Akt/PKB. NatCell Biol. 2009; 11(4):420-432.
20. Tang Y, Simoneau AR, Liao WX, Yi G, Hope C, Liu F, Li S, Xie J, Holcombe RF, Jurnak FA, Mercola D, Hoang BH and Zi X. WIF1, a Wnt pathway inhibitor, regulates SKP2 and c-myc expression leading to G1 arrest and growth inhibition of human invasive urinary bladder cancer cells. MolCancer Ther. 2009; 8(2):458-468.
21. Barre B and Perkins ND. The Skp2 promoter integrates signaling through the NF-kappaB, p53, and Akt/GSK3beta pathways to regulate autophagy and apoptosis. MolCell. 2010; 38(4):524-538.
22. Moro L, Arbini AA, Yao JL, di Sant'Agnese PA, Marra E and Greco M. Mitochondrial DNA depletion in prostate epithelial cells promotes anoikis resistance and invasion through activation of PI3K/Akt2. Cell DeathDiffer. 2009; 16(4):571-583.
23. Marian CO, Yang L, Zou YS, Gore C, Pong RC, Shay JW, Kabbani W, Hsieh JT and Raj GV. Evidence of epithelial to mesenchymal transition associated with

increased tumorigenic potential in an immortalized normal prostate epithelial cell line. Prostate. 2011; 71(6):626-636.

24. Xie D, Gore C, Liu J, Pong RC, Mason R, Hao G, Long M, Kabbani W, Yu L, Zhang H, Chen H, Sun X, Boothman DA, Min W and Hsieh JT. Role of DAB2IP in modulating epithelial-to-mesenchymal transition and prostate cancer metastasis. ProcNatlAcadSciUSA. 2010; 107(6):2485-2490.
25. Wu HC, Hsieh JT, Gleave ME, Brown NM, Pathak S and Chung LW. Derivation of androgen-independent human LNCaP prostatic cancer cell sublines: role of bone stromal cells. IntJCancer. 1994; 57(3):406-412.
26. Qiu GH, Xie H, Wheelhouse N, Harrison D, Chen GG, Salto-Tellez M, Lai P, Ross JA and Hooi SC. Differential expression of hDAB2IPA and hDAB2IPB in normal tissues and promoter methylation of hDAB2IPA in hepatocellular carcinoma. JHepatol. 2007; 46(4):655-663.
27. Yano M, Toyooka S, Tsukuda K, Dote H, Ouchida M, Hanabata T, Aoe M, Date H, Gazdar AF and Shimizu N. Aberrant promoter methylation of human DAB2 interactive protein (hDAB2IP) gene in lung cancers. IntJCancer. 2005; 113(1):59-66.
28. Dote H, Toyooka S, Tsukuda K, Yano M, Ouchida M, Doihara H, Suzuki M, Chen H, Hsieh JT, Gazdar AF and Shimizu N. Aberrant promoter methylation in human DAB2 interactive protein (hDAB2IP) gene in breast cancer. ClinCancer Res. 2004; 10(6):2082-2089.
29. Duggan D, Zheng SL, Knowlton M, Benitez D, Dimitrov L, Wiklund F, Robbins C, Isaacs SD, Cheng Y, Li G, Sun J, Chang BL, Marovich L, Wiley KE, Balter K, Stattin P, et al. Two genome-wide association studies of aggressive prostate cancer implicate putative prostate tumor suppressor gene DAB2IP. JNatlCancer Inst. 2007; 99(24):1836-1844.
30. Golledge J and Kuivaniemi H. Genetics of abdominal aortic aneurysm. CurrOpinCardiol. 2013; 28(3):290-296.
31. Gao D, Inuzuka H, Tseng A and Wei W. Akt finds its new path to regulate cell cycle through modulating Skp2 activity and its destruction by APC/Cdh1. Cell Div. 2009; 4:11.
32. Xie D, Gore C, Zhou J, Pong RC, Zhang H, Yu L, Vessella RL, Min W and Hsieh JT. DAB2IP coordinates both PI3K-Akt and ASK1 pathways for cell survival and apoptosis. ProcNatlAcadSciUSA. 2009; 106(47):19878-19883.
33. Hao B, Oehlmann S, Sowa ME, Harper JW and Pavletich NP. Structure of a Fbw7-Skp1-cyclin E complex: multisite-phosphorylated substrate recognition by SCF ubiquitin ligases. MolCell. 2007; 26(1):131-143.
34. Hao B, Zheng N, Schulman BA, Wu G, Miller JJ, Pagano M and Pavletich NP.

Structural basis of the Cks1-dependent recognition of p27(Kip1) by the SCF(Skp2) ubiquitin ligase. MolCell. 2005; 20(1):9-19.

35. Ravid T and Hochstrasser M. Diversity of degradation signals in the ubiquitin-proteasome system. NatRevMolCell Biol. 2008; 9(9):679-690.
36. Wirbelauer C, Sutterluty H, Blondel M, Gstaiger M, Peter M, Reymond F and Krek W. The F-box protein Skp2 is a ubiquitylation target of a Cul1-based core ubiquitin ligase complex: evidence for a role of Cul1 in the suppression of Skp2 expression in quiescent fibroblasts. EMBO J. 2000; 19(20):5362-5375.
37. Rodier G, Makris C, Coulombe P, Scime A, Nakayama K, Nakayama KI and Meloche S. p107 inhibits G1 to S phase progression by down-regulating expression of the F-box protein Skp2. JCell Biol. 2005; 168(1):55-66.
38. Bashir T, Dorrello NV, Amador V, Guardavaccaro D and Pagano M. Control of the SCF(Skp2-Cks1) ubiquitin ligase by the APC/C(Cdh1) ubiquitin ligase. Nature. 2004; 428(6979):190-193.
39. Arbini AA, Greco M, Yao JL, Bourne P, Marra E, Hsieh JT, di Sant'agnese PA and Moro L. Skp2 overexpression is associated with loss of BRCA2 protein in human prostate cancer. AmJPathol. 2011; 178(5):2367-2376.
40. Yang G, Ayala G, De MA, Tian W, Frolov A, Wheeler TM, Thompson TC and Harper JW. Elevated Skp2 protein expression in human prostate cancer: association with loss of the cyclin-dependent kinase inhibitor p27 and PTEN and with reduced recurrence-free survival. ClinCancer Res. 2002; 8(11):3419-3426.
41. Drobnjak M, Melamed J, Taneja S, Melzer K, Wieczorek R, Levinson B, Zeleniuch-Jacquotte A, Polsky D, Ferrara J, Perez-Soler R, Cordon-Cardo C, Pagano M and Osman I. Altered expression of p27 and Skp2 proteins in prostate cancer of African-American patients. ClinCancer Res. 2003; 9(7):2613-2619.
42. Luo D, He Y, Zhang H, Yu L, Chen H, Xu Z, Tang S, Urano F and Min W. AIP1 is critical in transducing IRE1-mediated endoplasmic reticulum stress response. JBiolChem. 2008; 283(18):11905-11912.
43. Zhang H, Zhang R, Luo Y, D'Alessio A, Pober JS and Min W. AIP1/DAB2IP, a novel member of the Ras-GAP family, transduces TRAF2-induced ASK1-JNK activation. JBiolChem. 2004; 279(43):44955-44965.
44. Laney JD and Hochstrasser M. (2011). Analysis of protein ubiquitination. Current Protocols in Protein Science, pp. 14.15.11-14.15.13.
45. Treier M, Staszewski LM and Bohmann D. Ubiquitin-dependent c-Jun degradation in vivo is mediated by the delta domain. Cell. 1994; 78(5):787-798.
46. McMahon M, Itoh K, Yamamoto M and Hayes JD. Keap1-dependent proteasomal degradation of transcription factor Nrf2 contributes to the negative regulation of antioxidant response element-driven gene expression. JBiolChem. 2003;

278(24):21592-21600.

47. Sato JD and Kan M. (2001). Media for culture of mammalian cells. Current Protocols in Cell Biology, pp. 1.2.1-1.2.15.
48. Taylor BS, Schultz N, Hieronymus H, Gopalan A, Xiao Y, Carver BS, Arora VK, Kaushik P, Cerami E, Reva B, Antipin Y, Mitsiades N, Landers T, Dolgalev I, Major JE, Wilson M, et al. Integrative genomic profiling of human prostate cancer. Cancer Cell. 2010; 18(1):11-22.
49. Tomlins SA, Mehra R, Rhodes DR, Cao X, Wang L, Dhanasekaran SM, Kalyana-Sundaram S, Wei JT, Rubin MA, Pienta KJ, Shah RB and Chinnaiyan AM. Integrative molecular concept modeling of prostate cancer progression. NatGenet. 2007; 39(1):41-51.
50. Wang Y, Xia XQ, Jia Z, Sawyers A, Yao H, Wang-Rodriquez J, Mercola D and McClelland M. In silico estimates of tissue components in surgical samples based on expression profiling data. Cancer Res. 2010; 70(16):6448-6455.
51. Casas E, Kim J, Bendesky A, Ohno-Machado L, Wolfe CJ and Yang J. Snail2 is an essential mediator of Twist1-induced epithelial mesenchymal transition and metastasis. Cancer Res. 2011; 71(1):245-254.

Figure legends

Figure 1 Inverse correlation between DAB2IP and Skp2 expression in prostatic cells.(A) Both DAB2IP and Skp2 expression were analyzed using western blot (upper panel) and their mRNA expression were determined using qRT-PCR (lower panel) in PNT1A (wide type, wt), ρ(0) and Cybrids. Data are represented as mean ± SEM. (B) Both DAB2IP and Skp2 protein expression were analyzed using western blot (upper panel) and their mRNA expression determined using qRT-PCR (lower panel) in PZ-HPV-7 and PZ-HPV-7T cells. Data represented as mean ± SEM. (C-F) PC3, PZ-HPV-7T, PNT1A wt, and 293J cells were transfected with incremental concentration of different plasmids. Cell lysates were subjected to western blot probed with DAB2IP or Skp2 antibody. The intensity of each band was measured using the Imaging-Pro Plus and normalized with Tubulin.

Figure 2 Regulation of DAB2IP expression by Skp2 mediated UPS (A) PNT1A wt, and ρ(0) cells were treated with MG132 (10 μM) for the indicated duration, and the DAB2IP expression was analyzed using western assays. The density of bands was measured using the Image-Pro plus and normalized with Tubulin. The fold of change [38] was calculated. Data are represented as mean ± SEM. (B) PNT1A ρ(0) cells were treated with or without MG132 (10 μM, 6 hours), IP with Skp2 or ubiquitin antibody, and probed with DAB2IP or p27 antibody. The intensity of each band was measured using the Image-Pro Plus and normalized with Tubulin. (C) Both DAB2IP and Skp2 expression in PZ-HPV-7T cells treated with MG132 at indicated concentration were analyzed using western blot. (D) The ubiquitinated DAB2IP was determined in PZ-HPV-7T cells using *in vivo*ubiquitination assay. Ubi. ISG-15, ubiquitin-like interferon stimulated gene (*ISG*)-15, was used as a negative control. (E) PC3 cells were treated with or without MG132, IP with Skp2 antibody or control IgG, and immunoblotted with DAB2IP or Skp2 antibody. The intensity of each band was measured using the Image-Pro Plus and normalized with Actin. (F) Endogenous Skp2 protein expression was determined in 293 wt and 293J cells using western blot. Actin was used for a loading control. (G) 293 J cells were transfected with indicated plasmids and treated with 10 μM MG132 for 6 hours. Cell lysates were subjected to western blot probed with DAB2IP, Skp2, or p27 antibody, or *in vivo* ubiquitination assay. (H) 293 wt cells were transfected with the indicated plasmids then both DAB2IP and Skp2 expression were determined with western blot.

Figure3 Determination of interactive domain in DAB2IP with Skp2 and its ubiquitination sites (A) Schematic representation of DAB2IP domain construct and the recognition sites of each antibody. (B-D) 293 wt or 293J cells were transfected

with a variety of DAB2IP domain constructs. Cell lysates were subjected to western blot or *in vivo* ubiquitination assay. * non-specific bands.

Figure4 The effect of DAB2IP on Skp2 protein expression mediated through Akt (A) 293J cells were transfected with plasmids carrying *DAB2IP* or *Skp2* cDNA for 48 hours. Cell lysates were IP with Skp2 antibody and immunoblotted with DAB2IP or Skp2 antibody (B-C) 293 wt or 293J were transfected with the indicated plasmids. Cell lysates were subjected to western blot, or *in vivo* ubiquitination assays, respectively. (D) Cell lysates were harvested from control (Con) or DAB2IP knocked-down (KD) cells of LAPC4, PZ-HPV-7 then subjected to western blot and Actin was used as a loading control. Both DAB2IP and Skp2 mRNA expression in LAPC4 KD, PZ-HPV-7 KD and their control cells were determined using qRT-PCR assays. Data are represented as mean +/- SEM. (E) PZ-HPV-7 KD and con cells were treated with cycloheximde (15 μg/ml) at indicated time. Cell lysates were subjected to western blot. The expression of GAPDH was used as a loading control. Skp2 degradation rate was determined based on Skp2/GAPDH ratios at each time point of cycloheximide treatment. (F) PZ-HPV-7 KD cells were treated with 10 μM LY294002 at indicated time. Cell lysates were subjected to western blot.

Figure 5 The effect of Skp2 on the tumor properties of prostatic cells from *in vitro* and *in vivo* (A) PZ-HPV-7 KD cells were transfected with control or Skp2 shRNA construct. DAB2IP and Skp2 expression were determined using western blot and actin was used as a loading control. One thousand cells/well were seeded using 96-well plate. *In vitro* cell growth was measured using MTT assays at the indicated time. Data are represented as mean +/- SEM. (B) PZ-HPV-7 KD cells and its control cells were plated on 24-well plate and the numbers of colony formation on soft agar were determined 2 weeks after plating. (C) PZ-HPV-7 KD cells and the control (1×10^6 cells) were injected into the nude mice subcutaneously and tumor take were determined at the indicated time. Each tumor was excised for histological examination. (D) The DAB2IP, Skp2, and p27 protein expression in LNCaP, C4-2, C4-2 shSkp2 and its control cells were determined using western blot. Both DAB2IP and Skp2 mRNA expression in C4-2 Skp2 shRNA and its control cells were determined using qRT-PCR assays. Data are represented as mean ± SEM. (E) 1×10^3 cells of C4-2 shSkp2 cells and its control were seeded at 96-well plate. *In vitro* cell growth was determined using MTT assays at the indicated time. Data are represented as mean +/- SEM. Twenty-four hours after the transfection of DAB2IP shRNA plasmids or control, C4-2 shSkp2 cells were seeded at 96-well plates then cell growth was determined using MTT assay. Data are represented as mean ± SEM.

Figure 6 The expression of DAB2IP and Skp2 in human PCa specimens (A) Three datasets of cDNA array from PCa patients were analyzed for the correlation between *DAB2IP* and *Skp2* mRNA expression. (B) Two tissue microarrays of PCa tissues were immunostained with DAB2IP Skp2 antibody. Right panel: the representative images were photographed and displayed. Left panel: the summary Table with sample number and percentage in parenthesis.

Supplementary Data

Figure A1 (A) Schematic representation of DAB2IP domain construct. (B, C) 293 wt or 293J cells were transfected with the indicated DAB2IP domain constructs. Cell lysates were subjected to western blot, or *in vivo* ubiquitination assay.

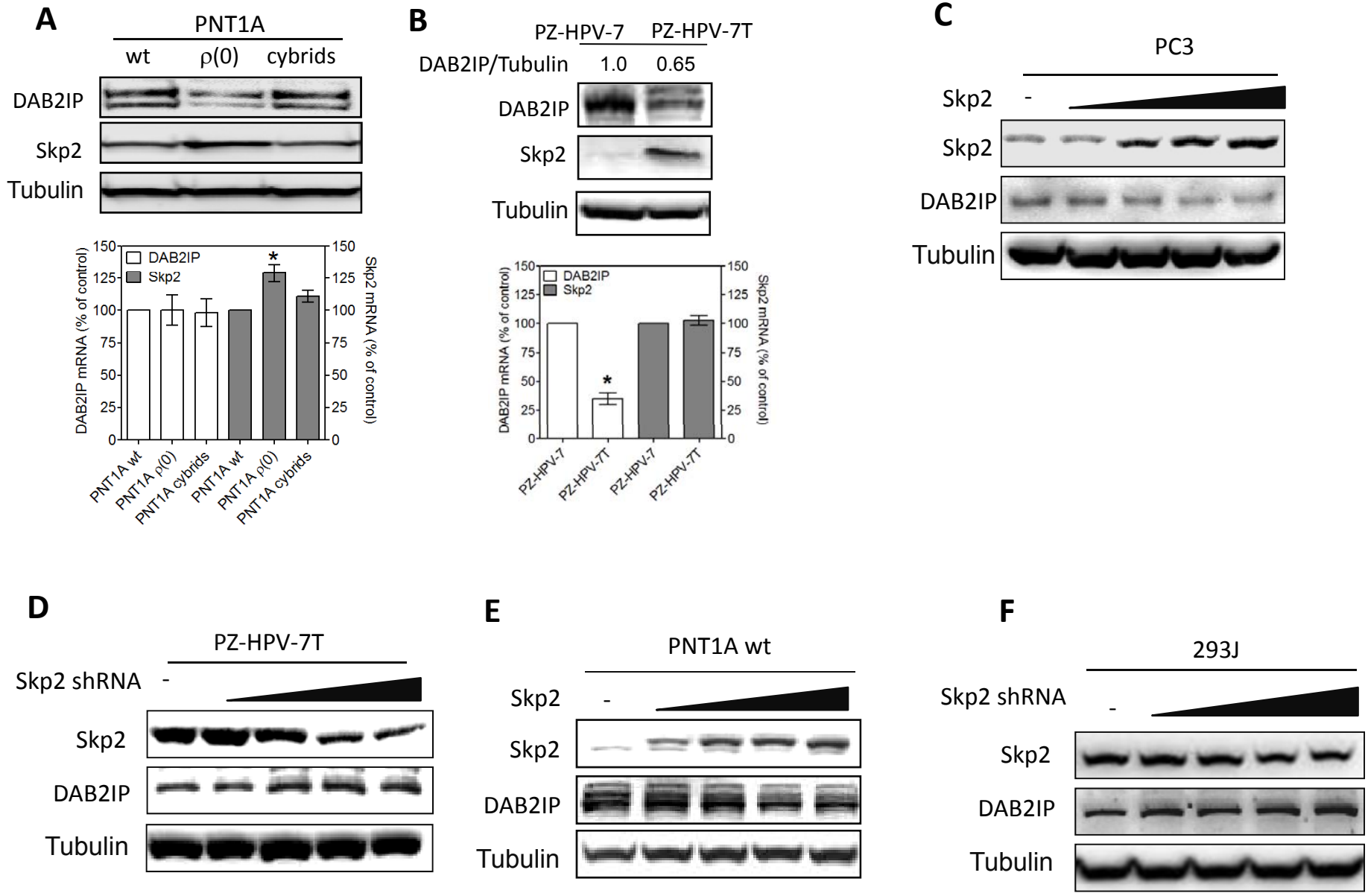
A
PNT1A
wt
ρ(0)
cybrids
DAB2IP
Skp2
Tubulin
DAB2IP mRNA (% of control)
Skp2 mRNA (% of control)
DAB2IP
Skp2
PNT1A wt
PNT1A ρ(0)
PNT1A cybrids
B
PZ-HPV-7
PZ-HPV-7T
DAB2IP/Tubulin
1.0
0.65
DAB2IP
Skp2
Tubulin
C
PC3
Skp2
DAB2IP
Tubulin
D
PZ-HPV-7T
Skp2 shRNA
Skp2
DAB2IP
Tubulin
E
PNT1A wt
Skp2
DAB2IP
Tubulin
F
293J
Skp2 shRNA
Skp2
DAB2IP
Tubulin

Fig. 1

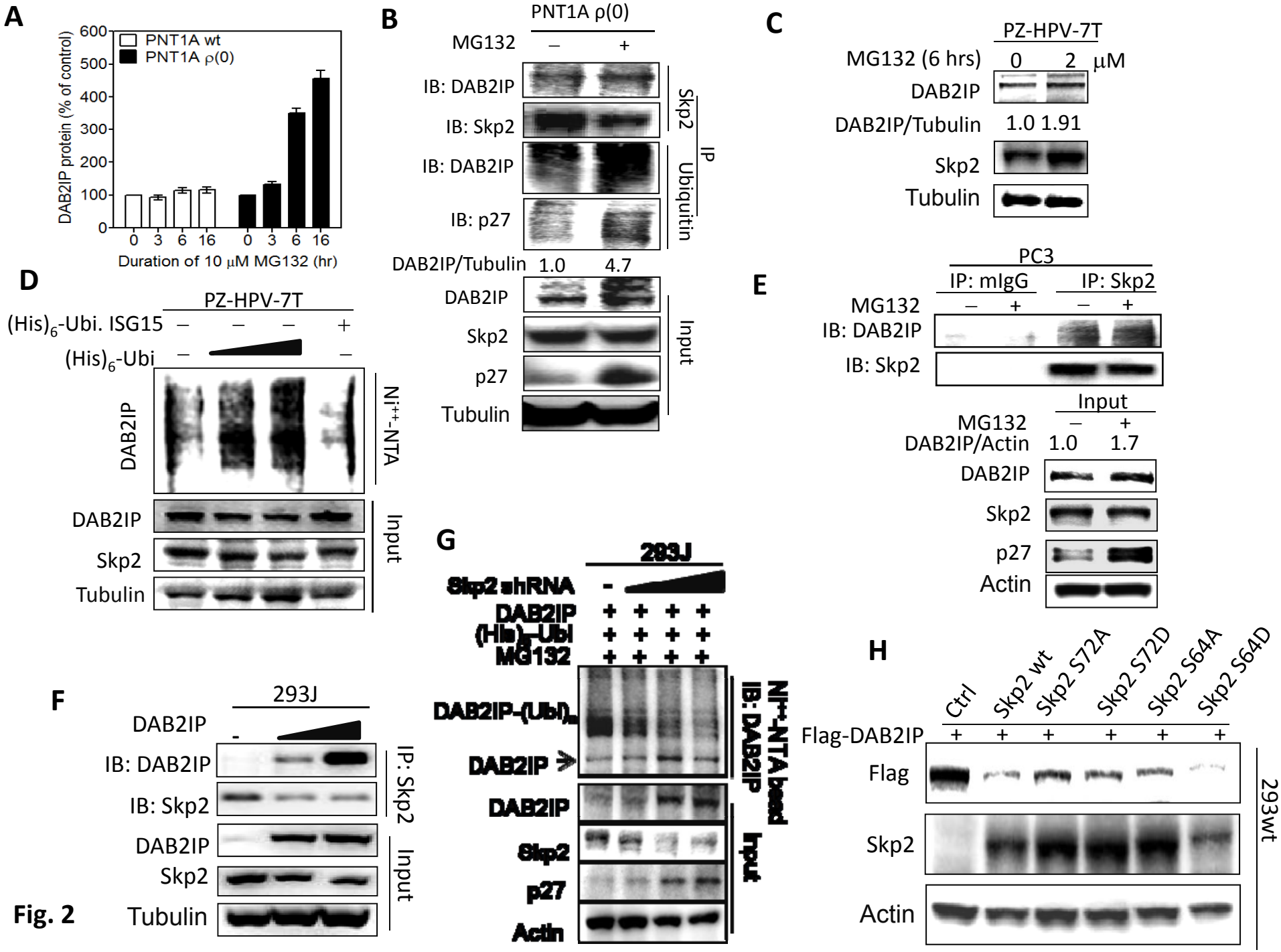
A
PNT1A wt
PNT1A ρ(0)
DAB2IP protein (% of control)
Duration of 10 μM MG132 (hr)
B
PNT1A ρ(0)
MG132
IB: DAB2IP
IB: Skp2
IB: DAB2IP
IB: p27
Skp2
Ubiquitin
IP
DAB2IP/Tubulin 1.0 4.7
DAB2IP
Skp2
p27
Tubulin
Input
C
PZ-HPV-7T
MG132 (6 hrs) 0 2 μM
DAB2IP
DAB2IP/Tubulin 1.0 1.91
Skp2
Tubulin
D
PZ-HPV-7T
(His)6-Ubi. ISG15
(His)6-Ubi
DAB2IP
Ni++-NTA
DAB2IP
Skp2
Tubulin
Input
E
PC3
IP: mIgG
IP: Skp2
MG132
IB: DAB2IP
IB: Skp2
Input
MG132
DAB2IP/Actin 1.0 1.7
DAB2IP
Skp2
p27
Actin
F
293J
DAB2IP
IB: DAB2IP
IB: Skp2
IP: Skp2
DAB2IP
Skp2
Tubulin
Input
G
293J
Skp2 shRNA
DAB2IP
(His)6-Ubi
MG132
DAB2IP-(Ubi)n
DAB2IP
Ni++-NTA beads
IB: DAB2IP
DAB2IP
Skp2
p27
Actin
Input
H
Ctrl
Skp2 wt
Skp2 S72A
Skp2 S72D
Skp2 S64A
Skp2 S64D
Flag-DAB2IP
Flag
Skp2
Actin
293wt

Fig. 2

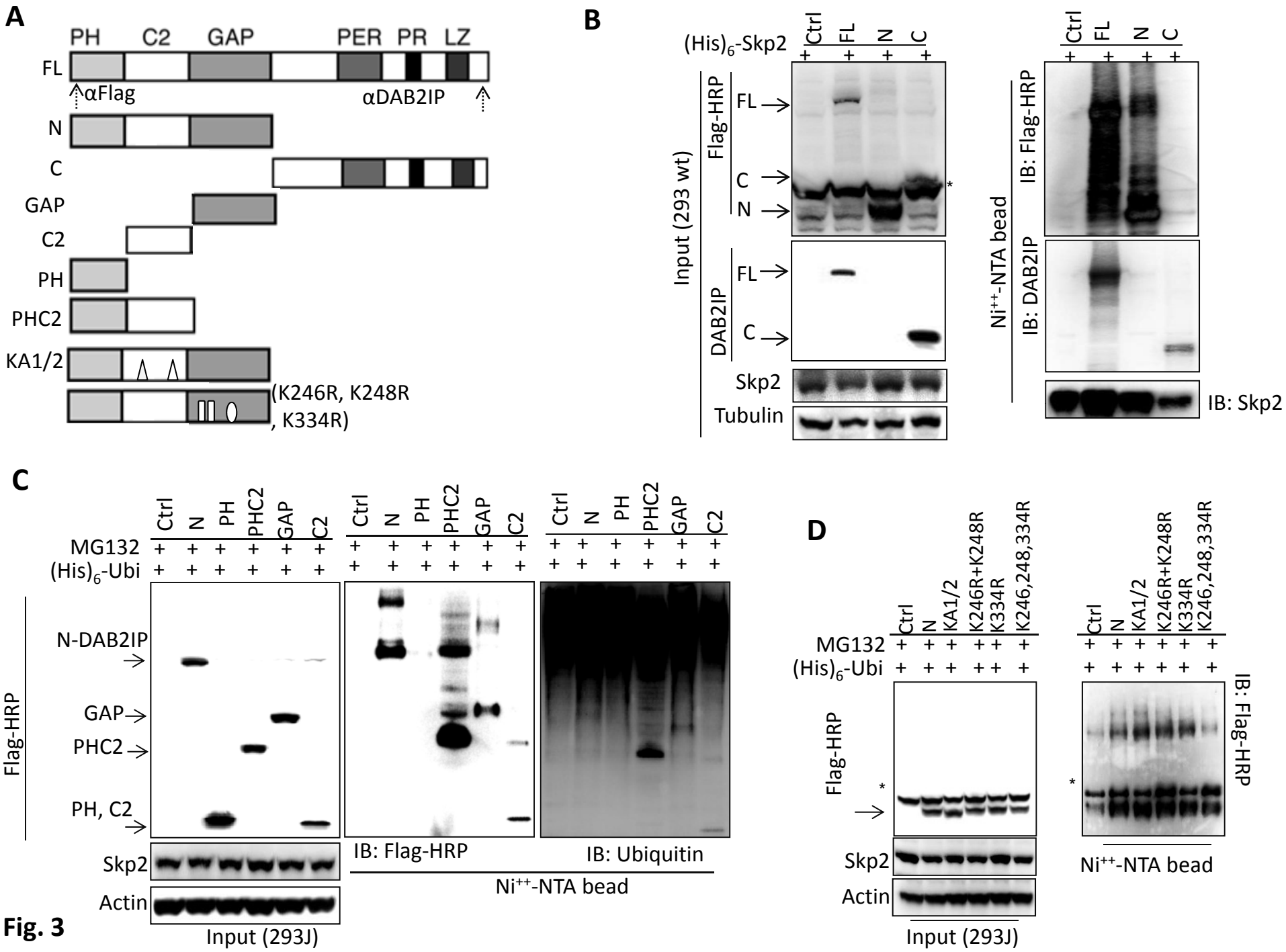
A
PH
C2
GAP
PER
PR
LZ
FL
αFlag
αDAB2IP
N
C
GAP
C2
PH
PHC2
KA1/2
(K246R, K248R
, K334R)
B
(His)6-Skp2
Ctrl
FL
N
C
Input (293 wt)
Flag-HRP
FL
C
N
DAB2IP
FL
C
Skp2
Tubulin
Ni++-NTA bead
IB: Flag-HRP
IB: DAB2IP
IB: Skp2
C
MG132
(His)6-Ubi
Ctrl
N
PH
PHC2
GAP
C2
Flag-HRP
N-DAB2IP
GAP
PHC2
PH, C2
Skp2
Actin
Input (293J)
IB: Flag-HRP
IB: Ubiquitin
Ni++-NTA bead
D
MG132
(His)6-Ubi
Ctrl
N
KA1/2
K246R+K248R
K334R
K246,248,334R
Flag-HRP
Skp2
Actin
Input (293J)
IB: Flag-HRP
Ni++-NTA bead

Fig. 3

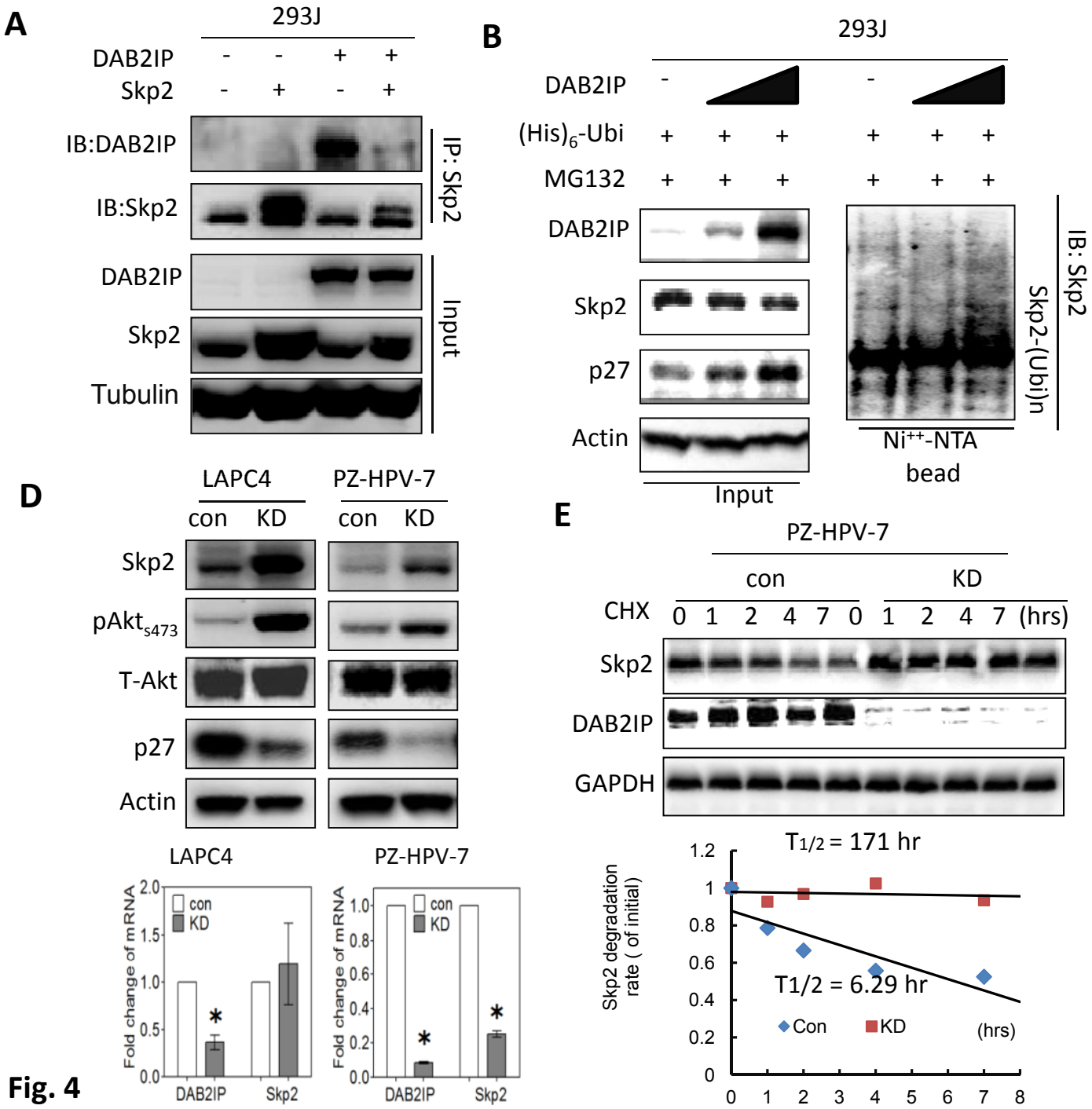
A
293J
DAB2IP
Skp2
IB:DAB2IP
IB:Skp2
IP: Skp2
DAB2IP
Skp2
Tubulin
Input
B
293J
DAB2IP
(His)6-Ubi
MG132
DAB2IP
Skp2
p27
Actin
Input
Ni++-NTA bead
Skp2-(Ubi)n
IB: Skp2
C
293 wt
Skp2
DAB2IP
Akt-CA
Skp2
DAB2IP
pAkts473
Actin
D
LAPC4
PZ-HPV-7
con
KD
Skp2
pAkts473
T-Akt
p27
Actin
LAPC4
PZ-HPV-7
Fold change of mRNA
con
KD
DAB2IP
Skp2
E
PZ-HPV-7
con
KD
CHX
0 1 2 4 7 0 1 2 4 7 (hrs)
Skp2
DAB2IP
GAPDH
T1/2 = 171 hr
Skp2 degradation rate (of initial)
T1/2 = 6.29 hr
Con
KD
(hrs)
F
(10μM)
LY294002
PZ-HPV-7 KD
0 3 6 9 12 24 (hrs
Skp2
pAkts473
T-Akt
GAPDH

Fig. 4

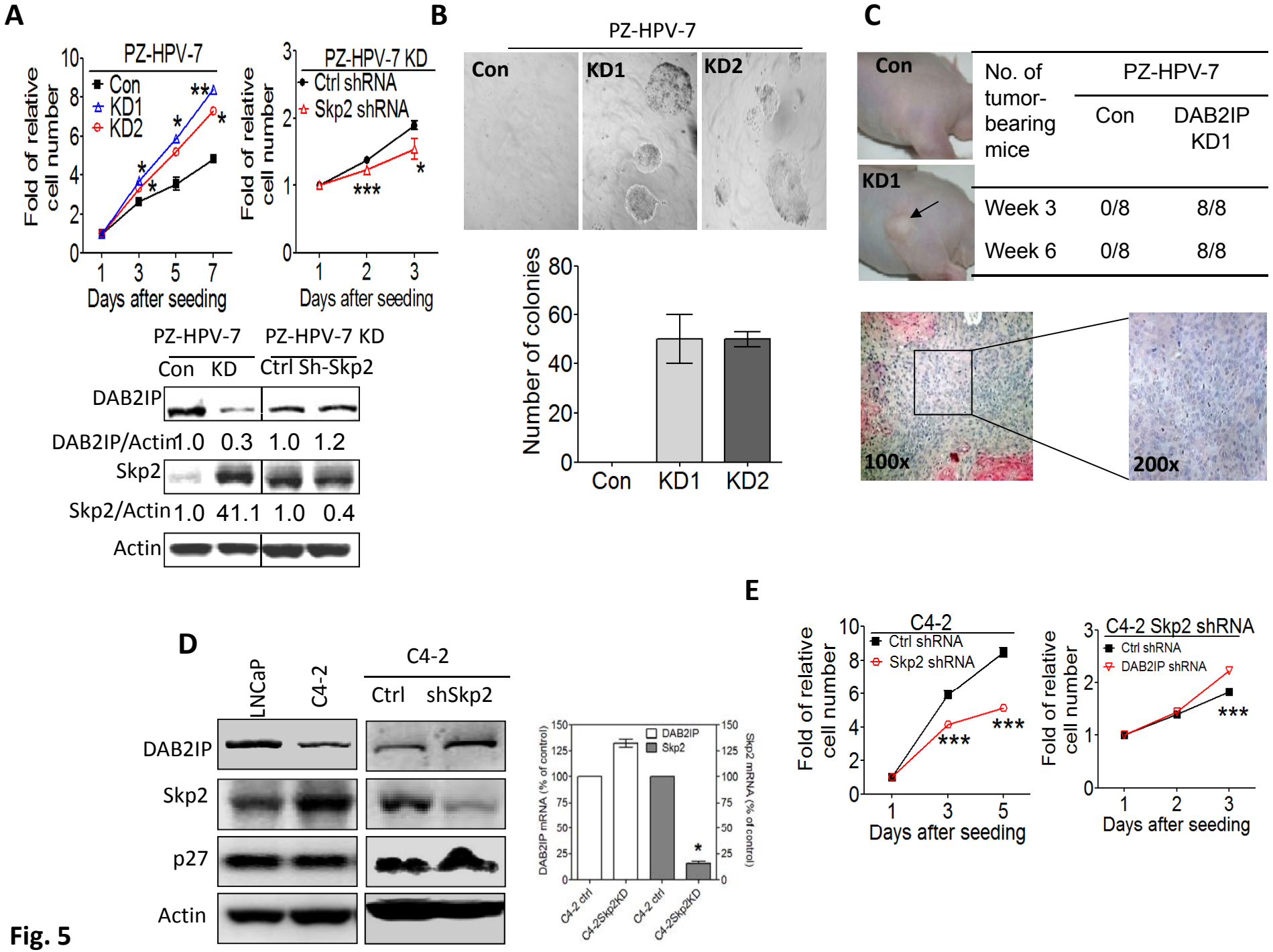
A
PZ-HPV-7
Con
KD1
KD2
Fold of relative cell number
Days after seeding
PZ-HPV-7 KD
Ctrl shRNA
Skp2 shRNA
PZ-HPV-7
PZ-HPV-7 KD
Con
KD
Ctrl
Sh-Skp2
DAB2IP
DAB2IP/Actin 1.0 0.3 1.0 1.2
Skp2
Skp2/Actin 1.0 41.1 1.0 0.4
Actin
B
PZ-HPV-7
Con
KD1
KD2
Number of colonies
C
Con
KD1
No. of tumor-bearing mice
PZ-HPV-7
Con
DAB2IP KD1
Week 3 0/8 8/8
Week 6 0/8 8/8
100x
200x
D
LNCaP
C4-2
C4-2
Ctrl
shSkp2
DAB2IP
Skp2
p27
Actin
DAB2IP mRNA (% of control)
Skp2 mRNA (% of control)
C4-2 ctrl
C4-2Skp2KD
C4-2 ctrl
C4-2Skp2KD
E
C4-2
Ctrl shRNA
Skp2 shRNA
Fold of relative cell number
Days after seeding
C4-2 Skp2 shRNA
Ctrl shRNA
DAB2IP shRNA
Fold of relative cell number
Days after seeding

Fig. 5

A

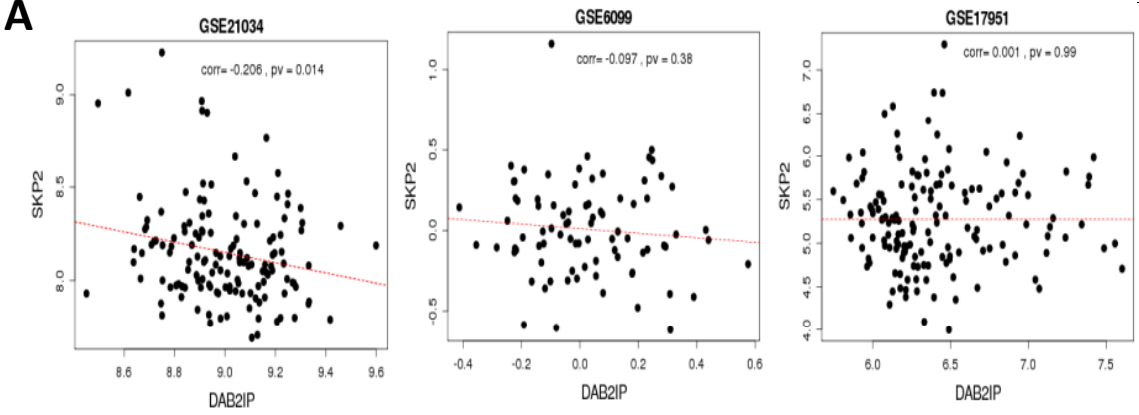

Meta-analysis, chisqure =10.49, DF=3, p-value: 0.105

Dataset	Corr. Coef.	*p*-value	% *
GSE21034 (n = 218)	-0.21	0.014	81.5
GSE17951 (n = 153)	0.001	0.989	52.84
GSE6099 (n = 83)	-0.10	0.380	71.19

B

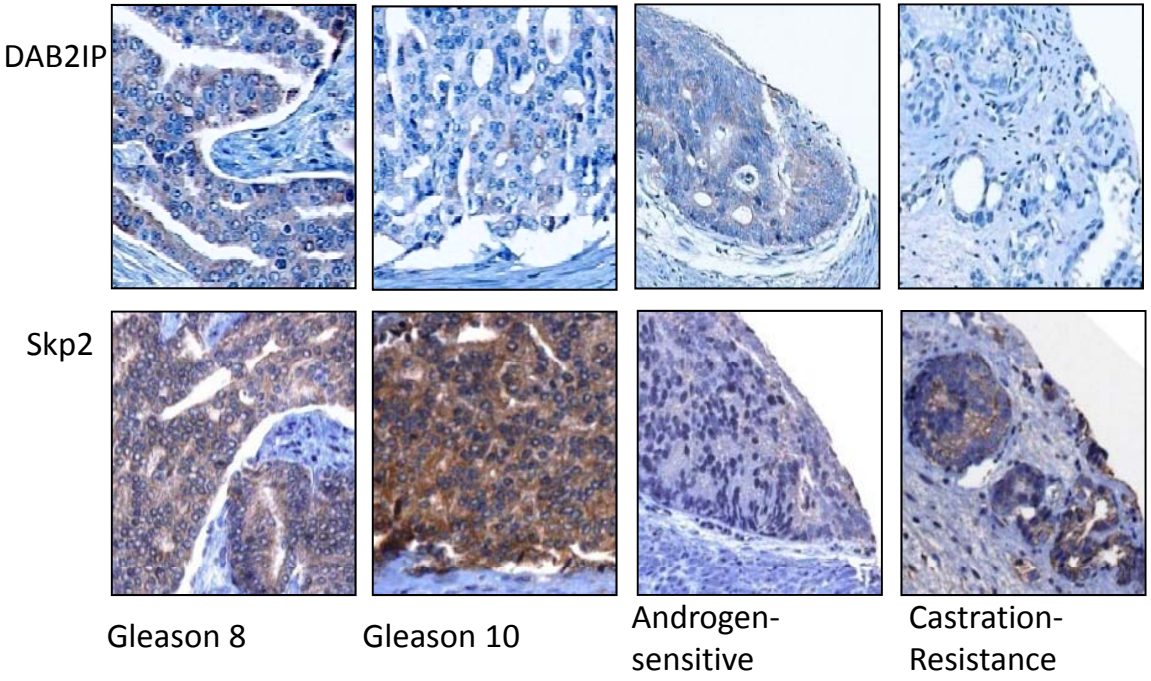

DAB2IP	**Skp2, n (%)**		
	Low	High	Total
Low	83 (31.6)	37 (14.1)	120 (45.7)
High	69 (26.2)	74 (28.1)	143 (54.3)
Total	152 (57.8)	111 (42.2)	263 (100)

Fig. 6

Appendices A.

Supplementary information

The sequences of primers for DAB2IP are 5'-TGGACGATGTGCTCTATGCC-3' (forward) and 5'-GGATGGTGATGGTTTGGTAG-3' (reverse). Primers for Skp2 are 5'-AGCCCGACAGTGAGAACATC-3' (forward) and 5'-GAAGGGAGTCCCATGAAACA-3' (reverse). Primers for 18S RNA are 5'-GGAATTGACGGAAGGGCACCACC-3' (forward) and 5'-GTGCAGCCCCGGACATCTAAGG-3' (reverse).

Figure A1 (A) Schematic representation of DAB2IP domain construct. (B, C) 293 wt or 293J cells were transfected with the indicated DAB2IP domain constructs. Cell lysates were subjected to western blot, or *in vivo* ubiquitination assay.

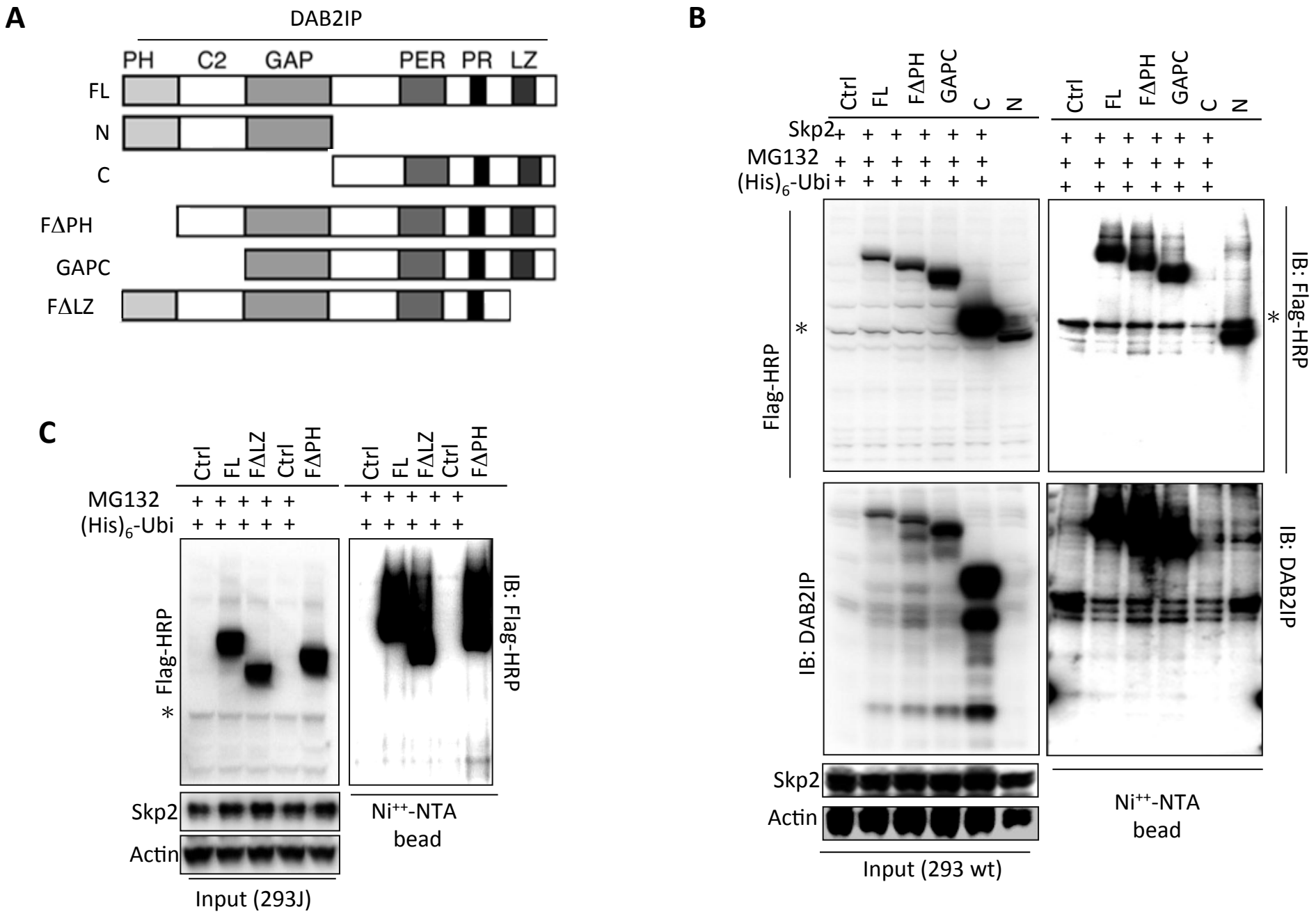
A
DAB2IP
PH
C2
GAP
PER
PR
LZ
FL
N
C
FΔPH
GAPC
FΔLZ
B
Ctrl
FL
FΔPH
GAPC
C
N
Skp2
MG132
(His)6-Ubi
Flag-HRP
IB: Flag-HRP
IB: DAB2IP
Skp2
Actin
Ni++-NTA bead
Input (293 wt)
C
Ctrl
FL
FΔLZ
FΔPH
MG132
(His)6-Ubi
Flag-HRP
IB: Flag-HRP
Skp2
Actin
Ni++-NTA bead
Input (293J)

Fig. A1